CD38 is a key regulator of enhanced NK cell immune responses during pregnancy through its role in immune synapse formation

Authors

Mathieu Le Gars[1,2,*], Christof Seiler[3], Alexander W. Kay[4], Nicholas L. Bayless[2], Elina Starosvetsky[5], Lindsay Moore[5], Shai S. Shen-Orr[5], Natali Aziz[6], Purvesh Khatri[1], Cornelia L. Dekker[3], Gary E. Swan[6], Mark M. Davis[7,8], Susan Holmes[4], Catherine A. Blish[1,2,9,*]

Departments of [1]Medicine, [4]Pediatrics, [6]Obstetrics & Gynecology, [7]Microbiology & Immunology, [2]Stanford Immunology Program, [6]Stanford Prevention Research Center, Stanford University School of Medicine, [3]Department of Statistics, Stanford University, Palo Alto, California; [5]Faculty of Medicine, Technion - Israel Institute of Technology, Israel; [8]Howard Hughes Medical Institute, [9]Chan Zuckerberg Biohub, San Francisco, California.

*Corresponding authors: Mathieu Le Gars, mlegars@stanford.edu and Catherine Blish, cblish@stanford.edu

Once sentence summary: CD38 is responsible for the enhanced immune responses of NK cells to influenza virus infection during pregnancy through immune synapse formation.

Abstract

Pregnant women are particularly susceptible to complications of influenza A virus infection, which may result from pregnancy-induced changes in the function of immune cells, including natural killer (NK) cells. To decipher mechanisms driving enhanced NK cell activity during pregnancy, we profiled NK cells from pregnant and non-pregnant women, which showed significantly increased CD38 expression during

pregnancy. CD38 expression defines a phenotypically distinct and mature subset of NK cells that display increased ability to secrete IFN-γ and to kill influenza-infected and tumor cells. This enhanced function is based on the ability of CD38 to promote the formation of the NK cell immune synapse. Thus, increased CD38 expression directly promotes enhanced NK cell responses during pregnancy through its role in immune synapse formation. These findings open new avenues in immunotherapeutic development for cancer and viruses by revealing a critical role for CD38 in the formation of the NK cell immune synapse.

Main text

Introduction

Pregnant women are at high-risk of complications from seasonal and pandemic influenza infections (*1*, *2*). During the 2009 H1N1 influenza virus pandemic, pregnant women in the United States suffered a disproportionately high mortality rate, accounting for 5% of deaths while representing only 1% of the total population (*3*). The majority of pregnant women who died of influenza-related illness during the pandemic were infected in the second and third trimesters of pregnancy (*4*). Influenza infection during second or third trimester of pregnancy is also associated with significant increases in miscarriages, stillbirths, and early neonatal diseases and death (*1*, *5*). However, the mechanisms behind this susceptibility to influenza infection during pregnancy are still poorly understood.

During pregnancy, the immune system has to finely balance its activity in order to tolerate semi-allogenic fetal antigens, while maintaining the ability to fight microbial challenges (*6-9*). These immune alterations may be at least partially responsible for the increased susceptibility of pregnant women to influenza virus (*10*, *11*). Recent studies have demonstrated enhanced responses to influenza virus by several innate immune cell subsets, including monocytes, dendritic cells and natural killer (NK) cells (*8*, *12-16*). In particular, NK cells play a critical role in virus clearance and regulation of the subsequent adaptive immune response to influenza virus (*17*, *18*). NK cells express an array of inhibitory receptors, including the killer-cell immunoglobulin-like receptors (KIRs) and the heterodimer NKG2A-CD94, and activating receptors, including NKp46, NKp30 and NKG2D, which together define their degree of maturation and responsiveness to stimuli (*19*, *20*). The expression of these receptors enables NK cells to sense altered cells, including virus-infected and cancerous cells *(21-23)*. In response to such threats, NK cells can produce cytokines, such as IFN-γ, which limits viral replication and tumor proliferation, and kill cells via release of cytolytic molecules or through engagement of death receptors. NK cell activation must be tightly regulated to limit tissue damage at the site of infection. The mechanisms by which NK cell activity is altered during

pregnancy are unknown but are particularly critical to balance protection from infection with the avoidance of a hyperinflammatory reaction that could cause irreversible injuries to the mother and the fetus.

The goal of our study was to identify pregnancy-mediated changes in NK cells and their impact on the immune response to influenza infection. Our prior study reported that NK cell responses to influenza virus-infected cells were enhanced during pregnancy (*12*). This finding may at least in part reflect the fact that virus infections were performed in bulk peripheral blood mononuclear cell (PBMC) cultures, where enhanced cytokine responses from monocytes and dendritic cells could have contributed to dramatic NK cell activation (*13*, *21*). In fact, NK cells from pregnant women stimulated directly with phorbol-myristate acetate and ionomycin in our experiments, or with IL-12/IL-15 by Kraus et al. (*15*), have suppressed responses compared to those of non-pregnant women. In this study, we aim to resolve these contradictory findings by determining the mechanisms behind changes in cell-intrinsic NK cell function during pregnancy. To do so, we used mass cytometry paired with logistic regression to predict pregnancy-related changes in NK cells between pregnant and non-pregnant women in two independent cohorts. We performed functional assays to define the role of specific NK cell receptors in the responsiveness to influenza-infected cells, uncovering a surprising new role for the cell surface molecule CD38 in the formation of the immune synapse that is required for NK cell cytotoxic activity. We then explored whether this phenomenon extended beyond the setting of influenza-infected cells and discovered that CD38 also promotes immune synapse formation between NK cells and cancer cells, potentially presenting new therapeutic targets in cancer and infectious diseases.

Results

NK cell immune response to influenza virus and cancer cells during pregnancy.

To investigate how pregnancy alters NK cell phenotype and function, we recruited two cohorts of pregnant and non-pregnant (control) women in subsequent years (Tables S1 and S2 for cohort 1 and 2 demographics). Pregnant women were enrolled in their second or third trimesters, and blood samples were collected at enrollment and 6 weeks postpartum. To investigate intrinsic NK cell function during pregnancy, NK cells and autologous monocytes were sorted from the PBMCs of controls (n=10), pregnant women (n=10), and postpartum women (n=10) from cohort 1 (Fig. 1A, experimental workflow). Monocytes were infected with 2009 pandemic H1N1 influenza virus strain and then co-cultured with the autologous NK cells before functional assessment by flow cytometry. We observed that the frequency of NK cells expressing CD107a as a marker of cytolytic activity (Fig. 1B) and IFN-γ production (Fig. 1C) was significantly greater in pregnant women than in controls or in postpartum women. These data confirm our earlier findings that influenza-specific NK cell responses are enhanced during pregnancy (*12*). However, monocytes demonstrate enhanced anti-influenza responses during pregnancy, which could activate NK cells through inflammatory cytokine production (*13*). We hypothesized that if NK cell function was intrinsically elevated during pregnancy, we should observe enhanced anti-tumor responses as well. We therefore exposed sorted NK cells from controls and pregnant women to the K562 tumor cell line (Fig. 1A), which represents a homogenous, identical target for NK cells from controls and pregnant women. NK cells from pregnant women demonstrated significantly greater CD107a expression and tumor cell killing than NK cells from non-pregnant women (Fig. 1, D and E). Interestingly, though tumor killing activity was enhanced during pregnancy, there were no significant differences in the frequency of IFN-γ-producing NK cells (Fig. 1F), possibly reflective of the lack of inflammatory cytokine production by these tumor targets. These data indicate that NK cells have an intrinsically enhanced ability to kill both infected and tumor targets during pregnancy.

Deep profiling of NK cell phenotype from healthy pregnant and non-pregnant women

To understand potential drivers of this enhanced NK cell function during pregnancy, we next profiled the expression patterns of inhibitory and activating surface receptors on NK cells in control non-pregnant women, pregnant women, and postpartum women. PBMCs from women in both cohorts were evaluated by mass cytometry as outlined in Fig. 2A and Tables S3 and S4 (antibody panels for cohort 1 and 2, respectively). NK cells were identified as $CD3^{-}CD19^{-}CD20^{-}CD14^{-}CD56^{+/-}CD16^{+/-}$ cells (Fig. S1A). The frequency of NK cells did not significantly differ between pregnant and control women, nor in pregnant vs. postpartum women in either cohort (Fig. S1, B and C). To identify NK cell markers predictive of pregnancy, we used a generalized linear model (GLM) with bootstrap resampling to account for correlations between cells and inter-individual variability (Figure 2A, and Materials and Methods). This method was selected because markers expressed on cells from the same subject are usually more highly correlated than marker expression patterns between subjects. Thus, accounting for correlated data reduces the number of false positives.

In both cohorts, the expression of CD38 was significantly predictive of pregnant vs. non-pregnant women (Fig. 2, B and C). CD38 also strongly predicted pregnancy in a paired comparison within women between their pregnant and post-partum time points (Fig. 2, D and E). To confirm these results, CD38 expression on NK cells was assessed by manual gating, revealing that NK cells from pregnant women express significantly more CD38 than NK cells from non-pregnant or postpartum women (Fig. S2, A to F). Several other markers, including PD-1, CD27, CD94, LILRB1, NKp46, NKp44, NKG2A, and CD244, were predictive of pregnancy in one of the cohorts or analyses (Fig. 2, B to E). Manual gating analyses similarly confirmed enhanced expression of several of these markers within individual cohorts and comparisons, yet none of the markers was consistently predictive of pregnancy across cohorts or analyses (Fig. S3 to S7). As CD38 was the only marker consistently predictive of pregnancy across both cohorts and all analyses, we elected to explore how its enhanced expression during pregnancy might alter NK cell function.

CD38 expression on NK cells correlates with the magnitude of the influenza-specific immune response

We assessed CD38 expression by conventional flow cytometry on NK cells during their response to influenza-infected cells as outlined in Fig. 1A. Consistent with our mass cytometry results, the frequency of CD38-expressing NK cells as well as the intensity of CD38 expression on NK cells was significantly greater in pregnant women compared to controls or postpartum women (Fig. 3, A and B). Further, CD38 expression was significantly correlated with the magnitude of the NK cell response as measured by CD107a expression (Fig. 3C) and IFN-γ production (Fig. 3D). This raises the possibility that the increased responses in pregnant women are driven primarily by their enhanced CD38 expression. We therefore evaluated the function of $CD38^-$ vs. $CD38^+$ NK cells. Regardless of pregnancy status, CD38-expressing NK cells displayed a higher CD107a and IFN-γ expression compared to $CD38^-$ NK cells (Fig. 3, E and F). These data are consistent with the idea that expansion of a highly functional subset of NK cell expressing CD38 is responsible for the enhanced influenza-specific NK cell responses during pregnancy.

To further confirm that CD38 expression is associated with enhanced NK cell responses to influenza regardless of pregnancy status, we used NK cells from healthy blood bank donors to compare the ability of $CD38^-$ versus total NK cells to respond to pH1N1-infected monocytes. We elected to compare $CD38^-$ NK cells to total NK cells (of which 45-95% express CD38, Fig. S2) rather than to sort on CD38 because its ligation could alter NK cell function. Total NK cells displayed significantly greater CD107a and IFN-γ responses to autologous influenza-infected monocytes than did $CD38^-$ NK cells (Fig. 3, G and H). Moreover, the frequency of dead monocytes was significantly increased after co-culture with total NK cells compared to $CD38^-$ NK cells, suggesting that $CD38^+$ NK cells are enhanced in killing activity (Fig. 3I). These data confirm that $CD38^+$ NK cells have increased responses to influenza-infected cells.

Profiling $CD38^-$ and $CD38^+$ NK cells.

To better understand the mechanisms driving enhanced function of CD38-expressing NK cells, we examined the phenotype of $CD38^+$ NK cells. We used GLM with bootstrap resampling to evaluate markers

predictive of CD38$^+$ vs. CD38$^-$ NK cells (Fig. 4A, for cohort 2 and fig. S8A, for cohort 1), which differed in the specific NK cell markers examined (Fig. 2A). As CD38 expression was associated with enhanced responsiveness in all subjects regardless of pregnancy status, we examined NK cells from both pregnant and control women together. We observed that CD38 expression marked a unique phenotype of NK cells in cohort 2 (Fig. 4A). Specifically, several activating (CD244 (2B4), CD11b, CD57, NKp30 and NKp46) and inhibitory (KIR2DL1, KIR2DL2/L3/S2, KIR3DL1, KIR3DL2 and LILRB1) receptors were significantly predictive of CD38$^+$ NK cells. CD38$^-$ NK cells were more likely to express CD94, CD27, and KIR2DL1. A similar analysis of cohort 1 confirmed the increased expression of CD57, NKp30 and NKp46 in CD38$^+$ NK cells compared to CD38$^-$ NK cells (Fig. S8A). Expression of perforin, which was not included in the panel to evaluate cohort 2, was significantly increased on CD38$^+$ NK cells (Fig. S8A). Manual gating to examine the frequency of NK cells expressing specific receptors, as well as their mean signal intensity, confirmed these results (Fig. 4, B and C). Similar results were obtained when the control and pregnant women were evaluated independently (Fig. S9, A and B). Overall, the increased expression of several KIRs, NKp30, NKp46, CD57, CD11b, and perforin suggest that CD38$^+$ NK cells are a mature subset with high cytotoxic potential.

CD38 plays a direct role in NK cell immune response to influenza infection.

The mature phenotype of CD38-expressing NK cells could explain their enhanced responsiveness if CD38 marks cells with greater functional potential. Yet it is also possible that CD38 plays a direct role in the NK cell immune response to influenza-infected cells. CD38 has two known functions, neither of which have been studied in antiviral or antitumoral NK cell function. First, it is an extracellular ectoenzyme that can drive intracellular calcium flux through i) catalyzing the synthesis of cyclic Adenosyl-di-phosphate ribose from Nicotinamide Adenine Dinucleotide$^+$ or ii) catalyzing the hydrolysis of cyclic Adenosyl-di-phosphate ribose into Adenosyl-di-phosphate ribose (*22*, *23*). Second, it is an adhesion molecule that binds to CD31 and likely other ligands (*24*, *25*). We therefore used an inhibitor of CD38 enzymatic activity, kuromanin,

to assess the role of CD38 enzymatic activity in the NK cell response to influenza-infected monocytes. We observed no significant differences in CD107a or IFN-γ responses in the presence or absence of this inhibitor at concentrations known to inhibit CD38 function in T cells (*26*) (Fig. S10, A and B). Thus, the enzymatic activity of CD38 does not appear to play a role in altering influenza-specific NK cell responses.

As monocytes express CD31 (Fig. S10C), we used CD38 and CD31 blocking antibodies to assess the role of CD38-CD31 interactions in the immune response to influenza. The addition of CD38 blocking antibodies significantly inhibited NK cell CD107a and IFN-γ responses (Fig. 5, A and B). Further, blocking CD38 diminished the frequency of dead monocytes, suggesting that NK cell killing is diminished (Fig. 5C). Blocking the CD38 ligand, CD31, also significantly abrogated NK cell CD107a and IFN-γ responses compared to the incubation with an isotype control antibody. These data indicate that CD38, in addition to marking a mature subset of NK cells, plays a direct role in NK cell responses to influenza, likely by the binding to its ligand, CD31.

CD38 is crucial to the establishment of immune synapse with influenza-infected cells.

We next investigated whether CD38-CD31 interactions might play a role in the formation of the immune synapse between the NK cell and the infected cell. We therefore examined whether CD38-CD31 interactions contributed to the ability of NK cells to make conjugates with influenza-infected monocytes. Conjugation between fluorophore-labelled NK cells and monocytes were assessed by flow cytometry (Fig. 5D and fig. S11). In presence of blocking antibodies to both CD38 and LFA-1 (which was used as a positive control), we observed a significant reduction in the formation of NK cell-monocyte conjugates compared to untreated cells or isotype control antibody-treated cells. This suggests that CD38 plays a role in immune synapse formation. To confirm this, using confocal microscopy, we observed that CD38 is co-localized with the adhesion molecule LFA-1 in the contact zone between NK cells and H1N1-infected monocytes (Fig. 5, E and F). Minimal accumulation of CD38 was observed when NK cells were in contact with mock-infected monocytes (Fig. 5, E and F). In presence of a blocking CD38 or CD31 antibody, the formation of

the immune synapse was strongly and significantly inhibited compared to non-treated cells or cells incubated with an isotype control antibody (Fig. 5, G and H). Similarly, immune synapse formation was rarely observed between H1N1-infected cells and $CD38^-$ NK cells. As a positive control, blocking LFA-1 also led to a significant decrease in the immune synapse formation between NK cells and pH1N1-infected monocytes compared to non-treated cells or cells treated with an isotype control antibody (Fig. 5, G and H). Together, these data indicate that CD38 contributes to the establishment of the immune synapse between NK cells and influenza-infected cells, which is pivotal for NK cell immune response.

CD38 contributes to immune synapse formation between NK cells and cancer cells.

To explore whether the role of CD38 in NK cell responses extends beyond the response to influenza-infected cells, we examined NK cell responses to K562 tumor cells. We exposed total or $CD38^-$ NK cells from healthy donors to K562 cancer cells in the presence of CD38 or CD31 blocking antibodies. Total NK cells had significantly greater CD107a responses than did $CD38^-$ NK cells and resulted in higher levels of tumor cell killing (Fig. 6, A and B). Blocking CD38 significantly diminished NK cell CD107a expression and tumor cell killing (Fig. 6, A and B). The frequency of IFN-γ^+ cells did not significantly differ between $CD38^-$ and total NK cells, and blocking CD38 and CD31 did not significantly alter the frequency of IFN-γ^+ NK cells responding to tumor targets (Fig. 6C). Blocking CD31 had no significant effect on CD107a expression, K562 cell death, or IFN-γ production, suggesting that an alternate ligand may be used. Thus, these data indicate that CD38 also plays a critical role in NK cell cytolytic responses to cancer cells. To demonstrate the direct role of CD38 in NK cell anti-tumor responses, we assessed NK cell-K562 cell conjugate formation, and found that blocking CD38 or LFA-1 (positive control) significantly diminished conjugate formation compared to isotype control or without antibody (Fig. 6D). Finally, we visualized CD38 in the formation of immune synapses between NK cells and K562 tumor cells. As depicted in Fig. 6, E and F, CD38 polarizes at the contact zone between NK cells and K562 cells. Together, our data indicate

227 that CD38 plays a crucial role in the establishment of the immune synapse and in NK cell cytotoxic function
228 towards cancer cells.

Discussion

During pregnancy, the maternal immune system is engaged in a fine balance: tolerance is required to preserve the fetus while defenses must be maintained to protect mother and baby from microbial challenges. NK cells play a critical role in this balance as their job is to patrol the body for 'altered self'(*27*). NK cell activity had been thought to be suppressed during pregnancy to protect the fetus (*28*), yet recent studies have suggested a more nuanced view. NK cells from pregnant women display diminished responses to stimulation with cytokines and phorbol-myristate acetate and ionomycin (*12*, *15*, *16*), yet NK cell responses to influenza-infected cells are enhanced (*12*). Here we profiled NK cells from pregnant and non-pregnant women to better understand how NK cell phenotype and function are altered during pregnancy. We discovered that pregnancy is characterized by increased expression of the multi-faceted surface protein CD38 on NK cells. CD38 is expressed on a large proportion of NK cells even in non-pregnant individuals and is significantly increased in cell surface density during pregnancy. $CD38^{+}$ NK cells display a mature phenotype and kill both infected and tumor cells more effectively than $CD38^{-}$ NK cells. The basis of this enhanced responsiveness is the ability of CD38 to promote immune synapse formation between NK cells and infected and tumor cells. These observations not only demonstrate a new role for CD38 in promoting NK cell functional responses through immune synapse formation, but also provide a mechanistic understanding of why NK cells display enhanced responses to influenza virus during pregnancy.

Pregnant women are significantly more likely to suffer adverse consequences from influenza infection than are the general population. During the 1918 influenza pandemic, the case fatality rate for influenza infection was estimated to be 27-75% among pregnant women but only 2-3% among the general population (*29*). Even with improved supportive care, the case-fatality rate among pregnant women was twice that of the general population during the 2009 pandemic (*3*). Thus, an understanding of the mechanisms driving this enhanced susceptibility to influenza infection during pregnancy represents an important challenge for the scientific community. During influenza virus infection, the recruitment of peripheral NK cells into the lungs

represents one of the first lines of defense following influenza infection (*30*). Though isolated NK cells stimulated with cytokines or chemicals have suppressed responses during pregnancy, our data here confirm earlier findings that NK cell responses to autologous influenza-infected cells are enhanced during pregnancy (*12*). This enhanced responsiveness could be deleterious to lung integrity and drive pathogenesis. Consistent with this idea, Kim and colleagues demonstrated that pregnant mice infected by influenza virus have an increased lung inflammation and damage compared to non-pregnant mice (*31*). Further, Littauer and colleagues suggested that innate immune responses play a role in the initiation of pregnancy complications such as pre-term birth and stillbirth following influenza virus infection (*10*). Finally, the idea that enhanced NK cell responses could be detrimental in pregnant women is consistent with observations that hyperinflammatory responses are a driving force behind severe influenza disease in humans (*32-34*). Thus, to better understand the potential contributions of NK cells to influenza pathogenesis during pregnancy, we sought to define exactly how pregnancy altered human NK cells.

We were surprised to discover that the most dramatic and consistent difference between NK cells of pregnant and non-pregnant women was an increase in CD38 expression during pregnancy. While CD38 is most commonly viewed as an activation marker on T cells, it is more highly expressed on NK cells and has several important functions. First, CD38 confers lymphocytes with the ability to adhere to endothelial cells through its binding to CD31, a necessary step in extravasation. CD38 also functions as an ectoenzyme, converting extracellular NAD^+ to cADPR through its cyclase activity or cADPR to Adenosyl-di-phosphate ribose through its hydrolase activity (*35*). These molecules in turn can diffuse into the cell and promote its activation by driving intracellular calcium increase, phosphorylation of signaling molecules, production of cytokines, and vesicular transport (*35*). The diverse roles and functions raised the question of whether increased CD38 expression during pregnancy is merely a marker of a more 'activated' state or whether it was playing a direct role in modulating NK cell function. Thus, we first explored whether CD38 expression marked a unique subset of NK cells. We found that expression of CD38 marks a population of NK cells

with a differential expression of KIRs, CD11b, CD57, perforin and CD94 compared to $CD38^-$ NK cells, indicating a higher degree of cell maturation (*36*). In particular, the high expression of one or several KIRs on $CD38^+$ NK cells is an essential feature characterizing NK cell maturation and terminal differentiation (*37*, *38*). This suggests that $CD38^+$ NK cells are functionally competent, with high cytotoxic abilities, but also likely self-tolerant since they display at least one inhibitory receptor for Major Histocompatibility Complex. The high degree of co-expression between KIR and CD38 could reflect a need to assure tolerance towards fetal semi-allogenic antigens, while maintaining a high degree of cytotoxicity towards virus-infected and transformed cells, as demonstrated here.

Our demonstration here that CD38 contributes to the formation of immune synapse between NK cells and their targets represents a novel role for this molecule. While much is known about its enzymatic activities and adhesion functions through interaction with CD31, CD38 has not been extensively studied in terms of the biology of immune cells, especially cytotoxic ones. We show here that CD38-CD31 interactions are necessary to establish the NK immune synapse and for its cytotoxic activity against influenza-infected target cells. Importantly, this function for CD38 was not restricted to NK cells role in responding to influenza-infected cells, as we also show that blocking CD38 diminishes the ability to kill tumor targets. Thus, CD38 has a previously unrecognized, but critical, role in facilitating cytolytic activity against both infected cells and tumor targets. Interestingly, blocking CD38 diminished both IFN-γ production and cytolytic activity in response to influenza-infected cells, but diminished only cytolytic activity, and not IFN-γ production, in response to K562 cells. This is likely due to a requirement for both cytokines (primarily type I interferons) and cellular contact to obtain maximal IFN-γ production by NK cells (Kronstad et al., in revision and bioRxiv). While infected monocytes produce abundant IFN-α, K562 cells do not.

This study leaves open the question of the mechanism by which CD38 is increased during pregnancy. CD38 protein expression increases with age (*39*). Our pregnant and non-pregnant women were well-matched for

age, so this cannot account for the differences between cohorts. CD38 gene and protein expression is regulated by transcription factors induced by diverse potential signals such as cytokines and hormones (*40*, *41*). Thus, the altered hormonal and inflammatory environments during pregnancy could contribute to enhanced CD38 expression. In particular, NK cells express the estrogen receptor beta (*42*). Estrogen binding to its receptor in peripheral NK cells could increase CD38 expression during pregnancy, especially during second and third trimester where a substantial increase in estrogen concentration in the blood is observed (*43*). While this has not been explored in humans or in pregnancy, CD38 protein expression on cardiomyocytes was increased following injection of systemic estrogen, but not progesterone, in a rat model (*41*).

Harnessing NK cell cytotoxic power has been of great interest within the scientific community within the last several years. Several studies suggest that CAR-modified NK cell immunotherapy may be as effective as CAR-T cells in recognizing and killing target cells after genetic modification (*44*, *45*). Thus, the identification of a new role for CD38 in immune synapse formation has significant implications for these therapies. For immunotherapy approaches in which cytotoxic activity is desired, it will be important to assure that these cells express CD38. Further, it will be important to understand the factors that control CD38 expression in vivo to assure its retention on effector cells. For instance, we find that both IL-2 and IL-15, two important cytokines for NK cell homeostasis, promote increased CD38 expression *in vitro* (data not shown). It is equally important that we assess the role of CD38 on $CD8^+$ cytotoxic T cells. Finally, our data raise interesting implications for the CD38-targeting agents that are currently in clinical use, primarily for multiple myeloma and chronic lymphocytic leukemia (*46*, *47*). Clinical treatment with daratumumab, a specific human CD38 binding antibody, improves patient outcomes (*46*), but also may lead to NK cell fratricide as most NK cells express CD38 (*48*, *49*). It is currently unclear how daratumumab affects CD38-mediated immune synapse formation, and how this influences NK cell killing. This will be an important area of future investigation.

There are several limitations of our study, including the fact that our mass cytometry panels differed between the two cohorts and remain limited to ~40 markers. Thus, we may have excluded other molecules involved in NK cell immune responses during pregnancy, including critical NK cell surface molecules such as DNAM-1, TIGIT and Siglec-7. We also did not follow-up on other differences that were seen in only one cohort. Further, here we studied peripheral blood NK cells and were not able to sample lung resident NK cells or uterine NK cells. Finally, we had limited data reflecting the prior history of the infected and control women in terms of their prior vaccination status, prior influenza infection status, cigarette and drug use, and others. We cannot exclude that unmeasured factors could influence the quality of the NK cell response to influenza.

Here, our goal was to better understand NK cell biology and activity in the context of pregnancy and influenza virus infection. Our work reveals that CD38 expression is increased on NK cells during pregnancy, and that CD38 marks a mature NK cell subset. Further, we demonstrate a novel role for CD38 in the enhancement of NK cell responses through its role in immune synapse formation. This new pathway controlling NK cell function could be used as a target in future therapeutics to modulate NK cell killing activity.

Materials and Methods

Study design

The goal of this study was to determine changes in the phenotype and function of NK cells during pregnancy. Two cohorts of pregnant women enrolled during their second and third trimester and control non-pregnant women were recruited in separate years. In cohort 1, twenty-one healthy pregnant women were recruited between October 2013 and March 2014 from the Obstetrics Clinic at Lucile Packard Children's Hospital at Stanford University. Twenty-one non-pregnant (control) women were recruited at Stanford's Clinical and Translational Research Unit (NCT number: NCT03020537, NCT03022422 and NCT02141581). In cohort 2, thirty-two non-pregnant (control) women were recruited at Stanford's Clinical and Translational Research Unit (NCT numbers: NCT01827462 and NCT03022422) and twenty-one healthy pregnant women were recruited between October 2012 and March 2013 from the Obstetrics Clinic at Lucile Packard Children's Hospital at Stanford University. No difference in terms of age has been observed in both cohort between control and pregnant women (*t test*: p=0.1967 for cohort 1; *t test*: p= 0.1697 for cohort 2). Venous blood was collected from all participants at baseline; pregnant women also provided a sample at six weeks postpartum. Participant criteria are listed in Supplemental Table S1 and S2. Exclusion criteria for all participants included concomitant illnesses, immunosuppressive medications, or receipt of blood products within the previous year. Pregnant women were also excluded for known fetal abnormalities and morbid obesity (pre-pregnancy body mass index > 40). This study was performed in accordance with the Declaration of Helsinki and approved by the Stanford University Institutional Review Board; written informed consent was obtained from all participants.

In addition, blood from healthy donors at the Stanford blood bank center was obtained to perform several functional assays in the study.

PBMC Isolation and cryopreservation

PBMCs from healthy donors and from individuals belonging to cohort 1 and 2 were isolated from whole blood by Ficoll-Paque (GE Healthcare) and cryopreserved in 90% fetal bovine serum (Thermo Scientific)/10% dimethyl sulfoxide (Sigma-Aldrich).

PBMC Staining and CyTOF Acquisition

Cryopreserved PBMCs from non-pregnant and pregnant women in cohort 1 and 2 were thawed and cells were transferred to 96-well deep-well plates (Sigma), resuspended in 25 μM cisplatin (Enzo Life Sciences) for 1 min and quenched with 100% serum. Cells were stained for 30 min on ice, fixed (BD FACS Lyse), permeabilized (BD FACS Perm II), and stained with intracellular antibodies for 45 min on ice. Staining panels are described in Tables S3 and S4. All antibodies were conjugated using MaxPar X8 labeling kits (DVS Sciences). Cells were suspended overnight in iridium interchelator (DVS Sciences) in 2% paraformaldehyde in phosphate-buffered saline (PBS) and washed 1× in PBS and 2× in H_2O immediately before acquisition on a CyTOF-1 (Fluidigm).

Preprocessing of Mass Cytometry Data

Prior to analysis, we transform protein counts using the inverse hyperbolic sine function. This transformation assumes a two-component model for the measurement error (*50*, *51*): small counts are less noisy than large counts. This model can be justified due to CyTOF2's dual count scale (CyTOF2 Mass Cytometer User Manual): less abundant proteins can be measured more precisely than high abundant proteins due to pulse overlap in the detector.

Generalized Linear Mixed Model

The response y_i specifies the experimental group for the i^{th} cell, e.g. encoding whether the cell i was stimulated ($y_i = 0$) or unstimulated ($y_i = 1$), and the explanatory variables are inverse hyperbolic sine

transformed protein counts $\boldsymbol{x}_i$. Each vector $\boldsymbol{x}_i$ is of length p equal to the number of measured proteins. Each experiment will produce n pairs of $(y_1, \boldsymbol{x}_1), \ldots, (y_n, \boldsymbol{x}_n)$ coming from different donors. Our statistical model is

$$y_i \sim \text{Bernoulli}(\pi_i)$$

$$\log\left(\frac{\pi_i}{1-\pi_i}\right) = \beta_{\text{donor}[i],0} + \sum_{j=1}^{p} \beta_{\text{donor}[i],j}\, x_{i,j} = \boldsymbol{\beta}^{\boldsymbol{T}}_{\text{donor}[i]} \boldsymbol{x}_i$$

$$\boldsymbol{\beta}_{\text{donor}[i]} \sim \text{Normal}(\boldsymbol{\theta}, \boldsymbol{\Sigma})\,.$$

In our notation for regression coefficients $\beta_{\text{donor}[i],j}$, the first subscript donor$[i]$ maps the i^{th} cell to its donor, and the second subscript indexes the j^{th} protein marker. We assume that the donor specific coefficients are distributed according to a multivariate normal distribution. This model is often called a Generalized Linear Mixed Model (GLMM). Using the GLMM terminology, the unknown parameters that we need to estimate are the fixed effects $\boldsymbol{\theta}$, the random effects $\boldsymbol{\beta}_{\text{donor}[i]}$, and the covariance matrix $\boldsymbol{\Sigma}$ of the random effect. GLMMs can account for donor specific heterogeneity by separating donor specific variation from overall variation. As it is common in single cell datasets, we observe 10,000 to 100,000 cells per donor and measure 30 to 40 proteins. To handle such large amounts of data, we use the R package *mbest* that implements a fast moment-based estimation to fit GLMM models (*52*). One key assumption in GLMMs is the modeling of random effects by a multivariate normal distribution.

Generalized Linear Model with Bootstrap Resampling

Our GLMM approach can be directly applied to paired experiments. In immunology, we often have a paired experimental design when comparing stimulated with unstimulated cells taken from the same blood sample. We also have paired samples, if we compare the functional response of different cell types within the sample blood sample. In contrast, in our pregnancy study, we have blood samples from pregnant and not pregnant donors. Furthermore, we do not have any additional covariates that we could use to match samples. In such

cases, the GLMM approach might provide conservative results, therefore, we propose to use a nonparametric bootstrap resampling (*53*) approach using standard Generalized Linear Models (GLMs) (*54*),

$$y_i \sim \text{Bernoulli}(\pi_i)$$

$$\log\left(\frac{\pi_i}{1-\pi_i}\right) = \beta_0 + \sum_{j=1}^{p} \beta_j \, x_{i,j} = \boldsymbol{\beta}^{\boldsymbol{T}} \boldsymbol{x}_i \, .$$

In this approach, we handle the donor heterogeneity without explicitly defining a parametric mixed effects distribution. One bootstrap draw is taken by sampling donors with replacement. For each bootstrap sample, we fit a GLM using the base R implementation. We repeat this procedure B times resulting in B coefficient vectors $\boldsymbol{\beta}_1^*, \ldots, \boldsymbol{\beta}_B^*$. We can then compute component-wise quantiles of these vectors to obtain confidence intervals.

R Package: CytoGLMM

All previously mentioned regression methods and additional exploratory data analysis tools are available in our new R package *CytoGLMM*.

The package can be installed from GitHub (https://github.com/ChristofSeiler/CytoGLMM).

Virus Preparation

A/California/7/2009 influenza (pH1N1) wild-type influenza A viruses obtained from Kanta Subbarao at the National Institutes of Health were propagated in embryonated chicken eggs.

Cell purification for functional assays

Cryopreserved PBMCs from healthy donors, or non-pregnant and pregnant women from cohort 1, were thawed and washed with complete RP10 media (RPMI 1640 (Invitrogen) supplemented with 10% fetal bovine serum (FBS), 2 mM L-glutamine, 100 U/ml penicillin, 100 mg/ml streptomycin (Life Technologies)) and 50 U/mL benzonase (EMD Millipore).

Cell isolation. Autologous NK cells and/or monocytes were purified by magnetic-activated cell sorting via negative selection (Miltenyi). In several experiments, $CD38^-$ NK cells were further isolated from total NK cells by magnetic-activated cell sorting via negative selection (Miltenyi).

Cell sorting. Autologous NK cells and/or monocytes were sorted using Sony sorter SH800 (Sony). The following antibodies were used to perform NK cell and monocyte sorting: CD3-Allophycocyanine (clone OKT3; BioLegend), CD14-Brilliant Violet 421 (clone HCD14; BioLegend), CD19-Alexa Fluor 488 (clone HIB19; Biolegend) and CD56-Phycoerythrin Cyanine 7 (clone NCAM; BioLegend).

Monocyte infection by influenza virus

Following isolation or purification, monocytes were washed and re-suspended in serum-free RPMI media at 1×10^5 per 100 μL and infected at a multiplicity of infection (MOI) of 3 for 1 h at 37°C with 5% carbon dioxide. One-hour post-infection, viral inoculum was removed and cells were re-suspended in 100 μL of complete RP10. Autologous NK cells were incubated separately for 5 min in Fc Block, washed, and incubated for 15 min with CD38 (clone AT1/3, Bio-Rad), CD31 (clone WM59, Biolegend) or LFA-1 (clone TS1/22, Invitrogen) blocking antibodies or isotype control antibodies. NK cells were then exposed to pH1N1-infected monocytes at a effector:target (E:T) ratio 1:1. After a further 2-hour incubation, 2 μM monensin, 3 μg/mL brefeldin A (eBiosciences), and anti-CD107a-allophycocyanin-H7 (BD Pharmingen) were added to the co-culture for 4 hours, followed by cell staining for flow cytometry analysis.

NK cell exposure to autologous K562 tumor cell line.

Following isolation or purification, NK cells were incubated for 5 min in Fc Block, washed, and incubated for 15 min with CD38, CD31 or LFA-1 blocking antibodies or isotype control antibodies. NK cells were then exposed to pH1N1-infected monocytes at a Effector:Target (E:T) ratio 1:1. Immediately following co-incubation, 2 μM monensin, 3 μg/mL brefeldin A, and anti-CD107a-allophycocyanin-H7 were added to the co-culture for 4 hours, followed by cell staining for flow cytometry analysis.

Cell staining and Flow-Cytometry Analysis

Cells were stained with LIVE/DEAD fixable Aqua Stain (Life Technologies), followed by surface staining and then fixed and permeabilized with FACS Lyse and FACS Perm II (BD Pharmingen) according to the manufacturer's instructions. Cells were stained with anti-CD3-PE or -APC, anti-CD16-PerCPCy5.5 (clone 3G8; BioLegend), anti-CD38-PE or FITC (clone HIT2 Biolegend), anti-IFNγ-FITC or V450 (clone B27; BD Biosciences), anti-CD56-PEcy7, or anti-CD14-APC or -APC-H7 and fixed using 1% paraformaldehyde. Uncompensated data were collected using a three-laser MACSQuant® Analyser (Miltenyi). Analysis and compensation were performed using FlowJo flow-cytometric analysis software, version 9.9.4 (Tree Star).

Confocal microscopy

Isolated NK cells were stained using CellTrace Violet dye (Thermofischer) for 20 min at RT then washed twice in PBS. Isolated NK and mock- or pH1N1-infected monocytes were incubated on a Poly-L-Lysine pre-coated 8 well μ-slide (Ibidi) for 2 hours (enough time to let the cells settle down). Cells were then washed in PBS-FBS 2%, fixed in PFA 4% for 15 min and washed twice in PBS-FBS 2%. Cells were then stained with mouse anti-CD38 and/or rabbit anti-LFA-1 antibody for 30 min at RT, then washed twice in PBS-FBS 2%. Secondary staining was performed using a goat anti-mouse AlexaFluor594 or a goat anti-rabbit AlexaFuor488 antibody for 30 min at RT. After washing the cells twice in PBS-FBS 2%, cell mount

491 media (Ibidi) was added on cells for microscopy. Images were acquired using LSM880 Meta (Zeiss) laser
492 scanning confocal microscope equipped with a 63× (NA 1.4) DIC oil objective.
493
494 *Flow cytometry-based conjugation assay*
495 Isolated NK cells were labeled with CellTrace CFSE for 20 min at 37°C, washed and incubated with Fc
496 Block for 5 min. NK cells were then incubated with no antibody, an isotype control or CD38 blocking
497 antibody for 15 min at 37°C. pH1N1-infected monocytes or K562 cells were labelled with CellTrace violet
498 for 20 min at RT. 10^5 NK cells and 2×10^5 target cells (E:T ratio 1:2) were mixed in 200 μl complete RP10,
499 incubated for the indicated times (0, 20 or 40 min) at 37°C, vortexed, and fixed with 1% PFA in PBS. Cell
500 mixtures were run on a three-laser MACSQuant® Analyser (Miltenyi). Analysis and compensation were
501 performed using FlowJo flow-cytometric analysis software, version 9.9.4 (Tree Star).
502
503 *Statistical Analysis*
504 Modeling was discussed above. Other statistical analyses were performed using GraphPad Prism, version
505 6.0d (GraphPad Software). Pregnant and control participant characteristics were compared using Mann–
506 Whitney *U* Tests for continuous variables and Fisher's exact test for discrete variables. Pregnant and
507 postpartum samples were compared using Wilcoxon match-paired test. Functional results were compared
508 between groups using Mann–Whitney *U* tests.
509

Supplementary Materials

Fig. S1Figure S1. NK cell gating strategy.

Fig S2. CD38 expression in control, pregnant and postpartum women from cohort 1 and 2.

Fig S3. Gating strategy for each marker on NK cells from cohort 1.

Fig S4. Gating strategy for each marker on NK cells from cohort 2.

Fig S5. Percentage of expression for each marker on NK cells from cohort 1 and 2 using conventional gating.

Fig S6. Mean Signal intensity of NK cell marker in control, pregnant and postpartum from cohort 1 using conventional gating.

Fig S7. Mean Signal intensity of NK cell marker in control, pregnant and postpartum from cohort 2 using conventional gating.

Fig S8. Comparison of $CD38^-$ and $CD38^+$ NK cell expression of each marker in control and pregnant women from cohort 1 using logistic regression model and conventional gating.

Fig S9. Comparison of activating and inhibitory receptor expression on $CD38^-$ and $CD38^+$ NK cells from cohort 2 in control or pregnant women by conventional gating.

Fig S10. Effect of the CD38 enzyme inhibitor, kuromanin, on the NK cell response to H1N1-infected monocytes.

Fig S11. CD38 contributes to NK cell - influenza-infected monocytes conjugation.

Table S1. Demographics for cohort 1.

Table S2. Demographics for cohort 2.

Table S3. Antibody panel for mass cytometry in cohort 1.

Table S4. Antibody panel for mass cytometry in cohort 2.

Acknowledgements: We thank our study volunteers for their participation in these studies, Sally Mackey for regulatory and data management, Sue Swope for consenting and conducting study visits and the staff of the Stanford Vaccine Program for overall study coordination.

Funding: This was supported by an Elizabeth and Russell Siegelman Fellowship in Infectious Diseases from the Stanford Child Health Research Institute (CHRI) to A.W.K., a Stanford CHRI postdoctoral fellowship to M.L.G., the CHRI – Stanford Clinical and Translational Science Award grant number UL1 TR000093 (A.W.K.), a National Institutes of Health (NIH) Training Grant: Viral Infections in Children T32 AI78896-05 (A.W.K.), a Smith Family Stanford Graduate Fellowship (N.L.B.), Ruth L. Kirschstein NRSA 1F31HD089675 (N.L.B.), a Clinical Scientist Development Award #2013099 from the Doris Duke Charitable Foundation (C.A.B.), the McCormick Faculty Award (C.A.B.), Tasha and John Morgridge Endowed Faculty Scholar in Pediatric Translational Medicine from Stanford CHRI and Stanford University School of Medicine (C.A.B.), an NIH Director's New Innovator Award DP2AI112193 (C.A.B.), an Infrastructure and Opportunity Fund (C.A.B.) as part of the Stanford Human Immunology Project Consortium (HIPC) Grant U19AI090019 (M.M.D.), and an investigator award from the Chan Zuckerberg Biohub (C.A.B.). Clinical cohorts were supported by NIH U19AI057229 (M.M.D.) and an NIH/NCRR CTSA award UL1 RR025744 (H. Greenberg).

Author contributions: M.L.G., A.W.K., N.L.B. and C.A.B. designed experiments. M.L.G., A.W.K. and N.L.B. conducted experiments. M.L.G. and C.S. analyzed the data. E.L., L.M., S.S.S.O., P.K., collaborated and provided advice in the analysis of the data. M.L.G and C.A.B. wrote the manuscript. M.M.D., C.L.D., G.E.S. and N.A. coordinated and provided human samples. M.M.D., C.S., and S.H. revised the manuscript.

Competing interests: All authors have no competing interests to declare.

558 **Data and materials availability:** Materials are available from the corresponding authors upon request.

559 All .FCS files will be uploaded to Immport upon publication.

560

561

562 **References and Notes:**

563 1. S. B. Omer, R. Bednarczyk, S. A. Madhi, K. P. Klugman, Benefits to mother and child of influenza
564 vaccination during pregnancy. *Human Vaccines & Immunotherapeutics*. **8**, 130–137 (2012).

565 2. R. S. Raj, E. A. Bonney, M. Phillippe, Influenza, immune system, and pregnancy. *Reprod Sci*. **21**, 1434–
566 1451 (2014).

567 3. Centers for Disease Control and Prevention (CDC), Estimates of deaths associated with seasonal
568 influenza --- United States, 1976-2007. *MMWR Morb. Mortal. Wkly. Rep*. **59**, 1057–1062 (2010).

569 4. A. M. Siston *et al*., Pandemic 2009 influenza A(H1N1) virus illness among pregnant women in the
570 United States. *JAMA*. **303**, 1517–1525 (2010).

571 5. C. Härtel *et al*., Preterm Birth during Influenza Season Is Associated with Adverse Outcome in Very
572 Low Birth Weight Infants. *Frontiers in Pediatrics*. **4**, 797 (2016).

573 6. A. Erlebacher, Immunology of the maternal-fetal interface. *Annual Review of Immunology*. **31**, 387–
574 411 (2013).

575 7. M. PrabhuDas *et al*., (Nature Publishing Group, 2015), vol. 16, pp. 328–334.

576 8. A. P. Kourtis, J. S. Read, D. J. Jamieson, Pregnancy and infection. *N. Engl. J. Med*. **371**, 1077–1077
577 (2014).

578 9. N. Periolo *et al*., Pregnant women infected with pandemic influenza A(H1N1)pdm09 virus showed
579 differential immune response correlated with disease severity. *J. Clin. Virol*. **64**, 52–58 (2015).

580 10. E. Q. Littauer *et al*., H1N1 influenza virus infection results in adverse pregnancy outcomes by disrupting
581 tissue-specific hormonal regulation. *PLoS Pathog*. **13**, e1006757 (2017).

582 11. M. Pazos, R. S. Sperling, T. M. Moran, T. A. Kraus, The influence of pregnancy on systemic immunity.
583 *Immunol. Res*. **54**, 254–261 (2012).

584 12. A. W. Kay *et al*., Enhanced natural killer-cell and T-cell responses to influenza A virus during
585 pregnancy. *Proc. Natl. Acad. Sci. U.S.A*. **111**, 14506–14511 (2014).

586 13. M. Le Gars *et al*., Increased Pro-Inflammatory Responses of Monocytes and Plasmacytoid Dendritic
587 Cells to Influenza A Virus Infection During Pregnancy. *J. Infect. Dis*. **214**, jiw448–1671 (2016).

588 14. N. Aghaeepour *et al*., An immune clock of human pregnancy. *Sci Immunol*. **2**, eaan2946 (2017).

589 15. T. A. Kraus *et al*., Characterizing the pregnancy immune phenotype: results of the viral immunity and
590 pregnancy (VIP) study. *J. Clin. Immunol*. **32**, 300–311 (2012).

591 16. T. A. Kraus *et al*., Peripheral blood cytokine profiling during pregnancy and post-partum periods. *Am.*
592 *J. Reprod. Immunol*. **64**, 411–426 (2010).

593 17. S. Stegemann-Koniszewski *et al*., Respiratory Influenza A Virus Infection Triggers Local and Systemic
594 Natural Killer Cell Activation via Toll-Like Receptor 7. *Front Immunol*. **9**, e46581 (2018).

595 18. S.-H. Lee, T. Miyagi, C. A. Biron, Keeping NK cells in highly regulated antiviral warfare. *Trends*
596 *Immunol*. **28**, 252–259 (2007).

19. E. Vivier, E. Tomasello, M. Baratin, T. Walzer, S. Ugolini, Functions of natural killer cells. *Nat. Immunol.* **9**, 503–510 (2008).

20. D. M. Strauss-Albee, A. Horowitz, P. Parham, C. A. Blish, Coordinated regulation of natural killer receptor expression in the maturing human immune system.

. *J. Immunol.* (2014).

21. E. Vendrame, J. Fukuyama, D. M. Strauss-Albee, S. Holmes, C. A. Blish, Mass Cytometry Analytical Approaches Reveal Cytokine-Induced Changes in Natural Killer Cells. *Cytometry Part B: Clinical Cytometry*. **92**, 57–67 (2017).

22. M. Howard *et al.*, Formation and hydrolysis of cyclic ADP-ribose catalyzed by lymphocyte antigen CD38. *Science*. **262**, 1056–1059 (1993).

23. S. Takasawa *et al.*, Synthesis and hydrolysis of cyclic ADP-ribose by human leukocyte antigen CD38 and inhibition of the hydrolysis by ATP. *J. Biol. Chem.* **268**, 26052–26054 (1993).

24. A. L. Horenstein, H. Stockinger, B. A. Imhof, F. Malavasi, CD38 binding to human myeloid cells is mediated by mouse and human CD31. *Biochem. J.* **330 (Pt 3)**, 1129–1135 (1998).

25. S. Deaglio *et al.*, CD38/CD31, a receptor/ligand system ruling adhesion and signaling in human leukocytes. *Chem. Immunol.* **75**, 99–120 (2000).

26. F. Morandi *et al.*, A non-canonical adenosinergic pathway led by CD38 in human melanoma cells induces suppression of T cell proliferation. *Oncotarget*. **6**, 25602–25618 (2015).

27. H. G. Hilton, P. Parham, Missing or altered self: human NK cell receptors that recognize HLA-C. *Immunogenetics*. **69**, 567–579 (2017).

28. A. P. Kourtis, J. S. Read, D. J. Jamieson, Pregnancy and infection. *N. Engl. J. Med.* **370**, 2211–2218 (2014).

29. S. A. Rasmussen, D. J. Jamieson, J. S. Bresee, Pandemic influenza and pregnant women. *Emerging Infect. Dis.* **14**, 95–100 (2008).

30. L. E. Carlin, E. A. Hemann, Z. R. Zacharias, J. W. Heusel, K. L. Legge, Natural Killer Cell Recruitment to the Lung During Influenza A Virus Infection Is Dependent on CXCR3, CCR5, and Virus Exposure Dose. *Front Immunol.* **9**, 781 (2018).

31. H. M. Kim, Y. M. Kang, B. M. Song, H. S. Kim, S. H. Seo, The 2009 pandemic H1N1 influenza virus is more pathogenic in pregnant mice than seasonal H1N1 influenza virus. *Viral Immunol.* **25**, 402–410 (2012).

32. C. Y. Cheung *et al.*, Induction of proinflammatory cytokines in human macrophages by influenza A (H5N1) viruses: a mechanism for the unusual severity of human disease? *Lancet*. **360**, 1831–1837 (2002).

33. D. Kobasa *et al.*, Aberrant innate immune response in lethal infection of macaques with the 1918 influenza virus. *Nature*. **445**, 319–323 (2007).

34. M. D. de Jong *et al.*, Fatal outcome of human influenza A (H5N1) is associated with high viral load and hypercytokinemia. *Nat. Med.* **12**, 1203–1207 (2006).

633 35. F. Malavasi *et al*., Evolution and function of the ADP ribosyl cyclase/CD38 gene family in physiology
634 and pathology. *Physiol. Rev.* **88**, 841–886 (2008).

635 36. M. Luetke-Eversloh, M. Killig, C. Romagnani, Signatures of human NK cell development and terminal
636 differentiation. *Front Immunol.* **4**, 499 (2013).

637 37. N. Anfossi *et al*., Human NK cell education by inhibitory receptors for MHC class I. *Immunity*. **25**,
638 331–342 (2006).

639 38. J. M. Elliott, W. M. Yokoyama, Unifying concepts of MHC-dependent natural killer cell education.
640 *Trends Immunol*. **32**, 364–372 (2011).

641 39. J. Camacho-Pereira *et al*., CD38 Dictates Age-Related NAD Decline and Mitochondrial Dysfunction
642 through an SIRT3-Dependent Mechanism. *Cell Metab*. **23**, 1127–1139 (2016).

643 40. S. Deaglio, T. Vaisitti, S. Aydin, E. Ferrero, F. Malavasi, In-tandem insight from basic science
644 combined with clinical research: CD38 as both marker and key component of the pathogenetic network
645 underlying chronic lymphocytic leukemia. *Blood*. **108**, 1135–1144 (2006).

646 41. S. Dogan *et al*., Estrogen increases CD38 gene expression and leads to differential regulation of
647 adenosine diphosphate (ADP)-ribosyl cyclase and cyclic ADP-ribose hydrolase activities in rat
648 myometrium. *Biol. Reprod*. **66**, 596–602 (2002).

649 42. M. Pierdominici *et al*., Estrogen receptor profiles in human peripheral blood lymphocytes. *Immunol.*
650 *Lett*. **132**, 79–85 (2010).

651 43. B. Polese *et al*., The Endocrine Milieu and CD4 T-Lymphocyte Polarization during Pregnancy. *Front*
652 *Endocrinol (Lausanne)*. **5**, 106 (2014).

653 44. D. Liu *et al*., Chimeric antigen receptor (CAR)-modified natural killer cell-based immunotherapy and
654 immunological synapse formation in cancer and HIV. *Protein Cell*. **8**, 861–877 (2017).

655 45. K. Rezvani, R. Rouce, E. Liu, E. Shpall, Engineering Natural Killer Cells for Cancer Immunotherapy.
656 *Mol. Ther*. **25**, 1769–1781 (2017).

657 46. H. M. Lokhorst *et al*., Targeting CD38 with Daratumumab Monotherapy in Multiple Myeloma. *N. Engl.*
658 *J. Med*. **373**, 1207–1219 (2015).

659 47. R. N. Damle *et al*., Ig V gene mutation status and CD38 expression as novel prognostic indicators in
660 chronic lymphocytic leukemia. *Blood*. **94**, 1840–1847 (1999).

661 48. K. A. Frerichs *et al*., CD38-targeting antibodies in multiple myeloma: mechanisms of action and clinical
662 experience. *Expert Rev Clin Immunol*. **14**, 197–206 (2018).

663 49. Y. Wang *et al*., Fratricide of NK Cells in Daratumumab Therapy for Multiple Myeloma Overcome by
664 Ex Vivo Expanded Autologous NK Cells. *Clin. Cancer Res*., clincanres.3117.2017 (2018).

665 50. D. M. Rocke, S. Lorenzato, A Two-Component Model for Measurement Error in Analytical Chemistry.
666 *Technometrics*. **37**, 176–184 (1995).

667 51. W. Huber, A. von Heydebreck, H. Sueltmann, A. Poustka, M. Vingron, Parameter estimation for the
668 calibration and variance stabilization of microarray data. *Stat Appl Genet Mol Biol*. **2**, Article3 (2003).

669 52. P. O. Perry, Fast moment-based estimation for hierarchical models. *Journal of the Royal Statistical*
670 *Society: Series B (Statistical Methodology)*. **79**, 267–291 (2016).

671 53. B. Efron, R. J. Tibshirani, in *An Introduction to the Bootstrap* (Springer US, Boston, MA, 1993), pp. 1–
672 9.

673 54. P. McCullagh, J. A. Nelder, *Generalized Linear Models* (Springer US, Boston, MA, 1989).

674

675 **Figures**

676 **Figure 1. NK cell immune response to influenza infected and tumor cells during pregnancy.**

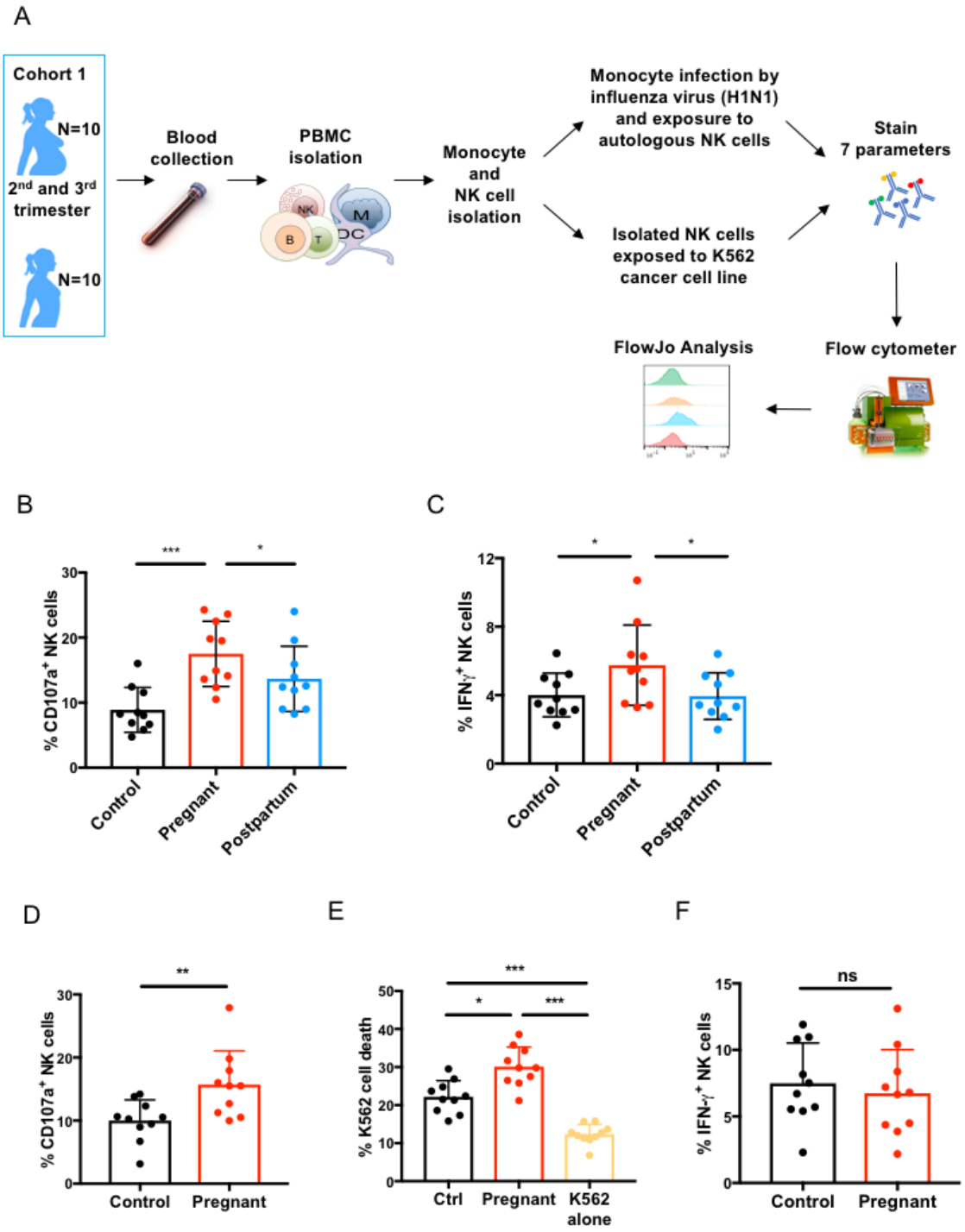

677

678 **(A)** Experimental workflow: PBMCs from controls (N=10), pregnant women (N=10) and postpartum
679 women (N=10) in cohort 1 were isolated from blood samples. Monocytes and NK cells were sorted and
680 monocytes were infected with the H1N1 influenza virus strain. NK cells were either exposed to H1N1-
681 infected monocytes or to K562 tumor cells for 7h or 4h, respectively. The NK cell immune response was

682 then determined by flow cytometry. (B) The frequency of **(B)** CD107a- and **(C)** IFN-γ-expressing NK cells
683 in response to influenza-infected monocytes. **(D)** The frequency of CD107a-expressing NK cells in
684 response to K562 cells. **(E)** The frequency of dead K562 cells as assessed by viability stain following co-
685 culture with NK cells. **(F)** The frequency of IFN-γ-production NK cells in response to K562 cells. *P<0.05,
686 **P<0.01 and ***P<0.001 (Mann–Whitney *U* Tests to compare controls vs. pregnant and control vs.
687 postpartum; Wilcoxon matched-paired test to compare pregnant vs. postpartum).
688

689 **Figure 2. Deep profiling NK cells in non-pregnant and pregnant women.**

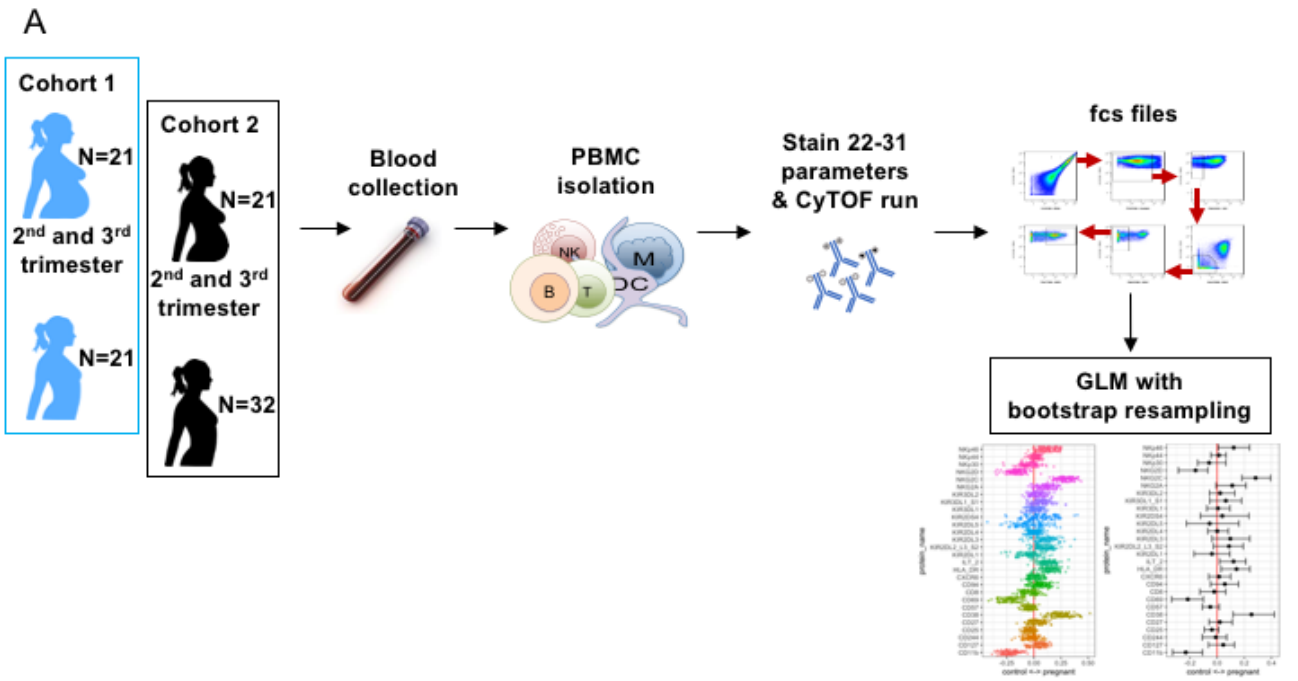

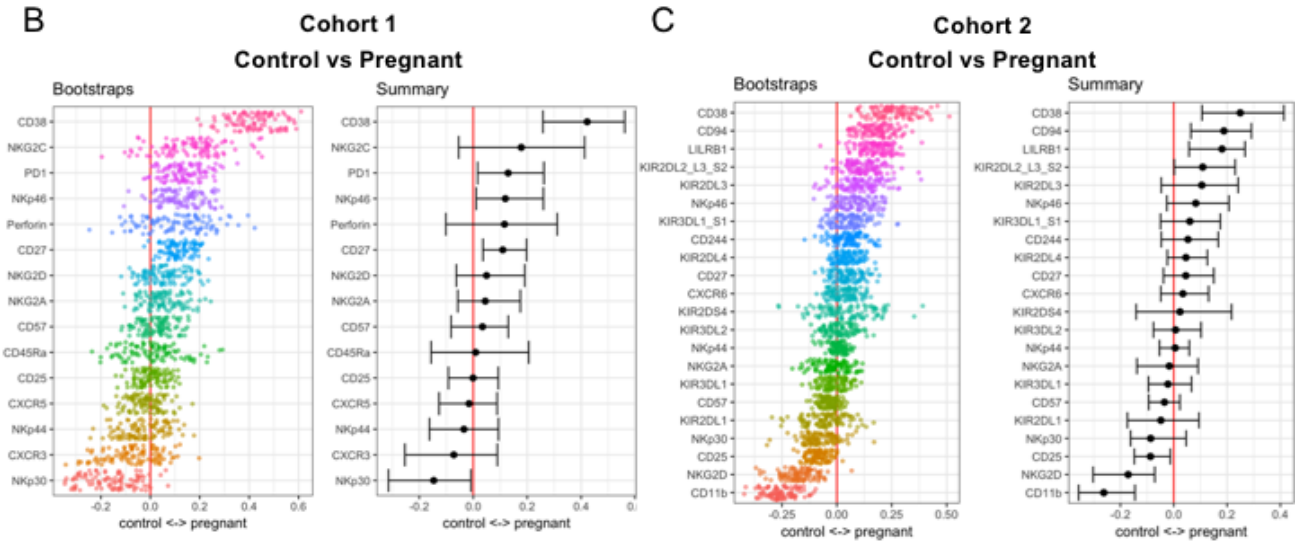

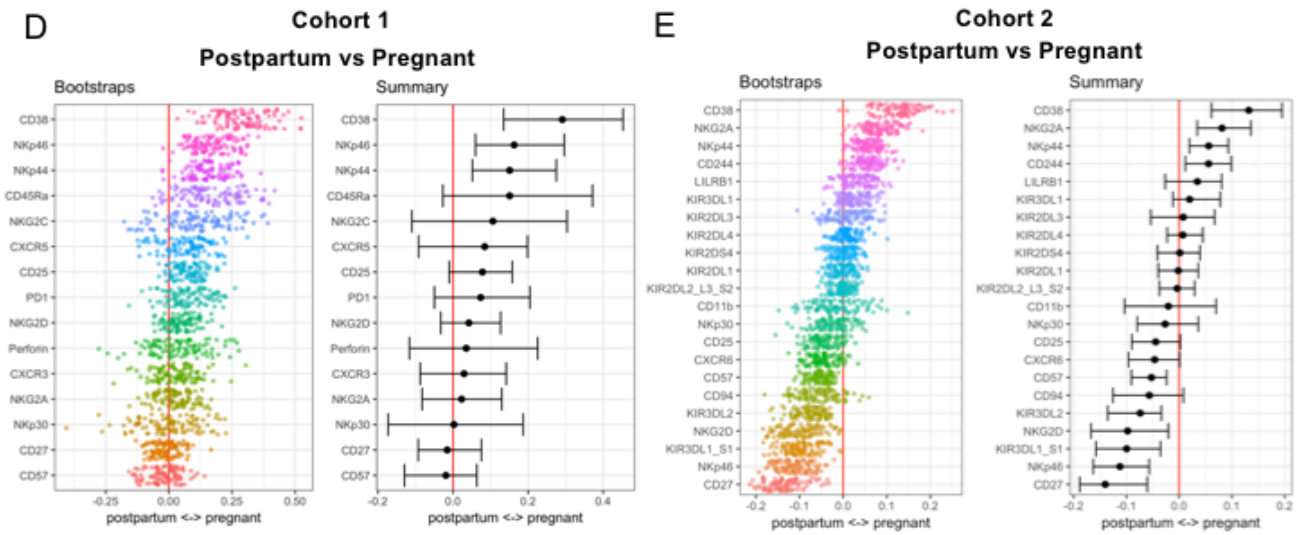

690

691 **(A)** Experimental workflow. PBMCs from controls, pregnant, and postpartum women were isolated and
692 labeled using a 22- or 31-parameter antibody panel for cohort 1 and 2, respectively. **(B)** Markers predictive
693 of control vs. pregnant women in Cohort 1 were assessed by GLM with bootstrap resampling. The markers
694 are listed on the y-axis and the x-axis represents the log-odds that the marker expression levels predict the
695 outcome (pregnancy on the left vs. control on the right). Dots in the left graph represent individual bootstrap
696 samples, with summary data in the right panel showing the 95% confidence interval. Markers in which the
697 bar does not cross zero are significantly predictive of one state vs. the other with a false discovery rate of
698 5%. **(C)** Evaluation of markers predictive of pregnancy vs. postpartum in cohort 1. **(D)** Markers predictive
699 of pregnancy vs. control and **(E)** pregnant vs. postpartum in cohort 2.
700
701

Figure 3. NK cell immune response to influenza virus infection in non-pregnant, pregnant women and postpartum.

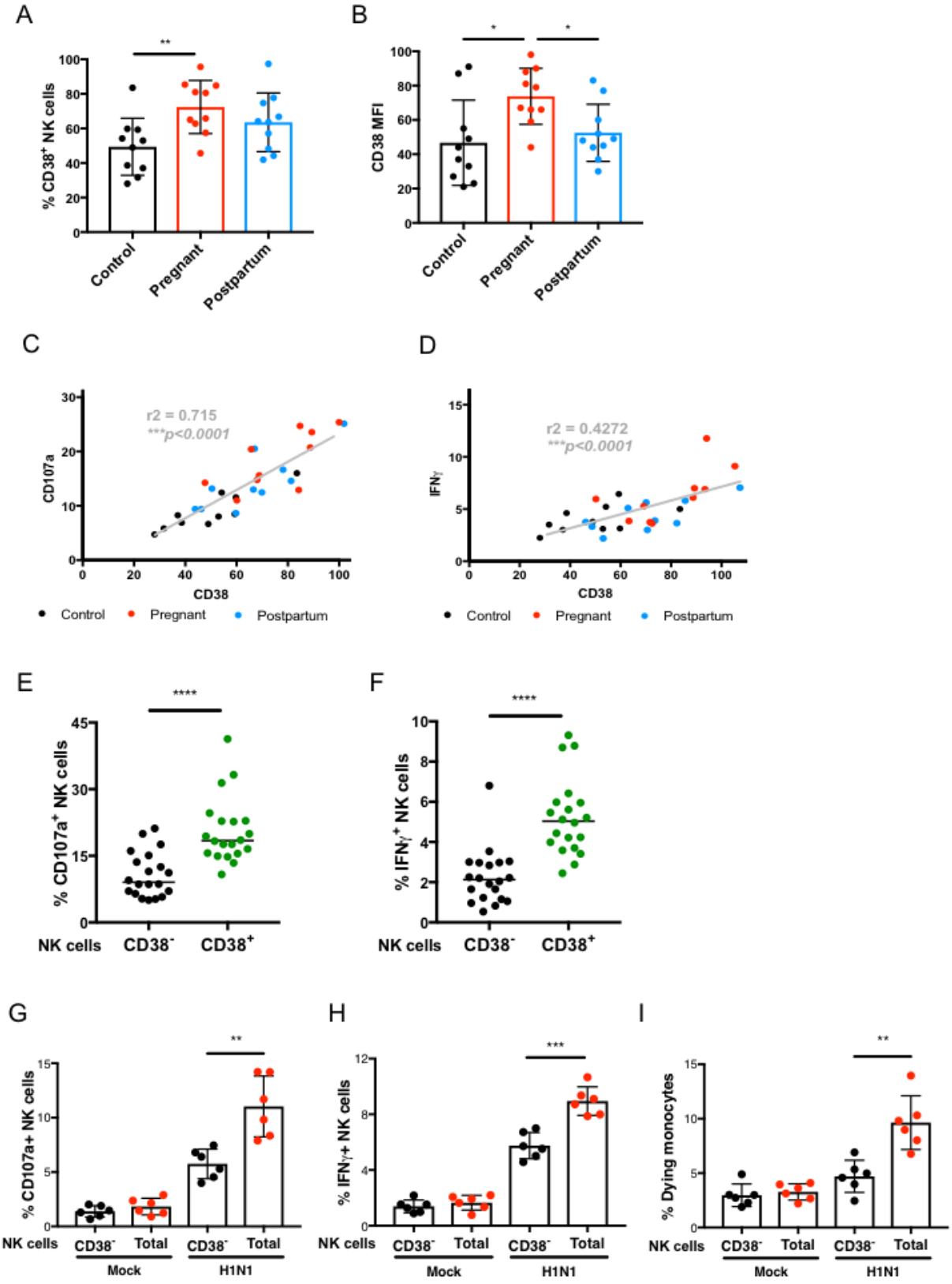

NK cells and autologous monocytes were sorted from the PBMCs of controls (N=10), pregnant women (N=10) and postpartum women (N=10). Monocytes were infected by H1N1 influenza virus and exposed to autologous NK cells for 7h. The frequency of NK cells expressing CD38 **(A)** and the CD38 MFI **(B)** on NK cells is shown. **P<0.01 (Mann–Whitney *U* Tests to compare controls vs. pregnant). Correlation by linear regression between CD38 and CD107a expression **(C)** or IFN-γ expression **(D)** was determined on NK cells. **(E)** CD107a expression and **(F)** IFN-γ production were measured in $CD38^-$ and $CD38^+$ subsets of NK cells exposed to autologous influenza-infected monocytes. Data from both pregnant and control women together were analyzed. **(G, H and I)** $CD38^-$ and total NK cells, and autologous monocytes were isolated from healthy blood donors (N=6). Monocytes were infected by H1N1 virus and exposed to autologous $CD38^-$ or total NK cells for 7h. CD107a expression **(G)** and IFN-γ production **(H)** by $CD38^-$ or total NK cells were determined by flow cytometry as well as monocyte cell death **(I)** as measured by a viability stain. ****P<0.0001 (Wilcoxon matched-paired test to compare $CD38^-$ NK cells vs. $CD38^+$ NK cells).

718 **Figure 4. Deep profiling of CD38$^-$ and CD38$^+$ NK cells in control and pregnant women.**

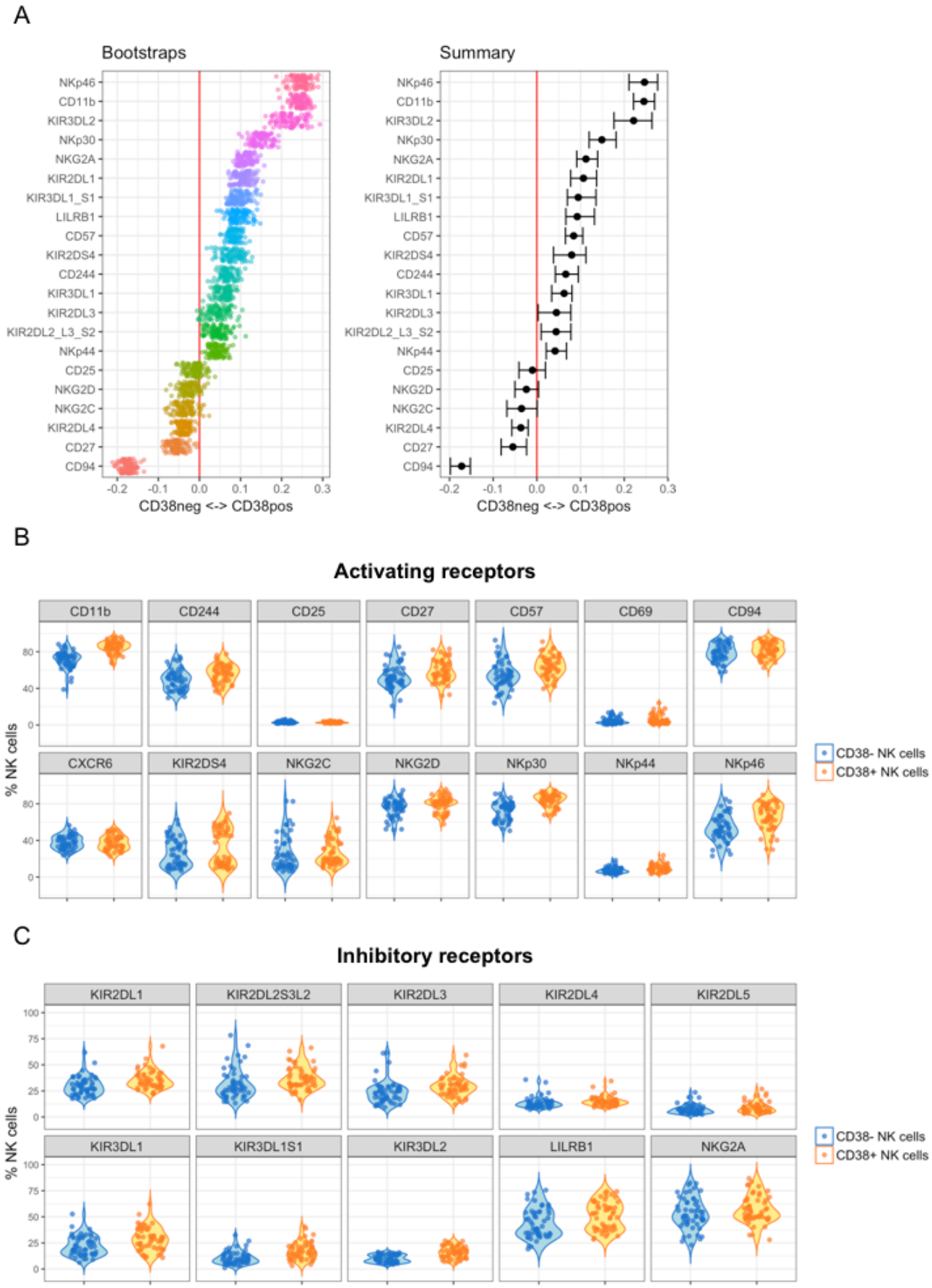

719

720 PMBCs from controls and pregnant women in cohort 2 were isolated and labeled using a 31-parameter
721 antibody panel (see Table S3). $CD38^-$ and $CD38^+$ NK cells were separated by manual gating and analyzed
722 using GLM with bootstrap resampling **(A)** and conventional gating strategy for each marker (**B**, for
723 activating receptor expression, and **C**, for inhibitory receptor expression).
724

Figure 5. CD38 contributes to the immune synapse between NK cells and H1N1-infected cells.

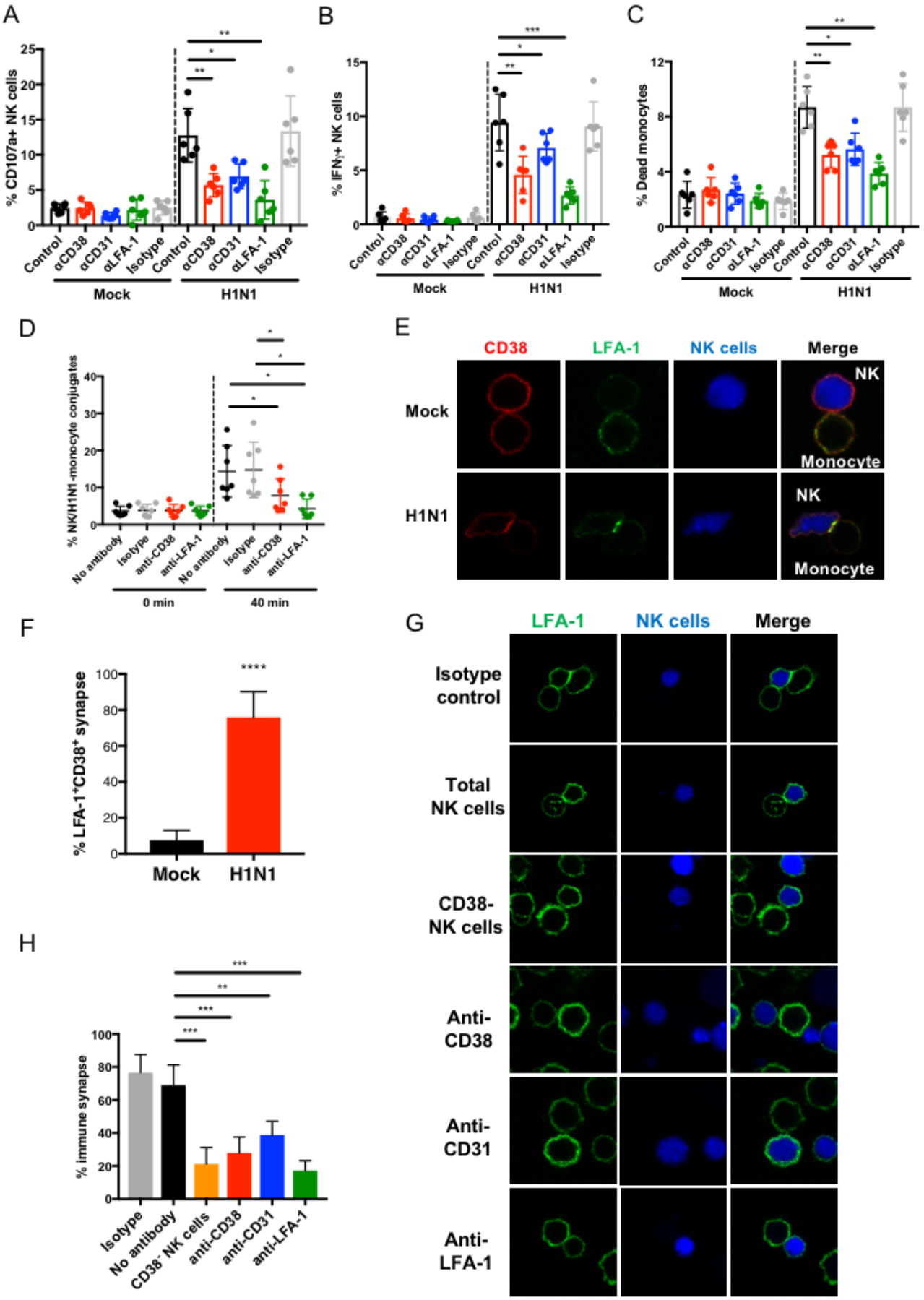

(A to C) Isolated NK cells from healthy donors (N=6) were exposed to autologous H1N1-infected monocytes in presence or absence of an isotype control antibody (grey dots) or a CD38 (red dots), CD31 (blue dots) or LFA-1 (green dots) blocking antibody or not (black dots). CD107a expression **(A)**, monocyte killing **(B)** and IFN-γ production **(C)** by NK cells were measured by flow cytometry. *P<0.05, **P<0.01, ***P<0.001 (Wilcoxon matched-paired test). **(D)** Conjugate formation was assessed by labeling NK cells with and monocytes with Cell Trace Violet. Monocytes were infected with H1N1 influenza and exposed to autologous NK cells for 0 or 40 min in presence or absence of a CD38 or LFA-1 blocking antibody or an isotype control antibody. NK cell-monocyte conjugation was determined by the accumulation of the double positive $CFSE^{+}$Cell Trace $Violet^{+}$ population by flow cytometry. *P<0.05 and **P<0.01 (Wilcoxon matched-paired test to compare each condition). **(E and F)** Total NK cells and monocytes from healthy blood donors (N=8) were isolated, monocytes were either mock- or H1N1-infected and exposed to autologous NK cells. **(E)** CD38 (in red) and LFA-1 (in green) localization was determined by confocal microscopy. A representative image is depicted for each condition. **(F)** Immune synapse formation was determined by the accumulation of LFA-1 at the contact zone (N=30) between NK cells (in blue) and mock- or H1N1-infected monocytes, and CD38 co-localization at the immune synapse was quantified. The percentage of immune synapses with co-localization is represented based on blinded counting. ****P<0.0001 (Wilcoxon matched-paired test). **(G and H)** H1N1-infected monocytes were exposed to $CD38^{-}$ NK cells or total NK cells in presence or absence of an isotype control, CD38, CD31 or LFA-1 blocking antibody. The accumulation of LFA-1 (in green) was measured to evaluate the number of immune synapses **(G)**. A representative image is depicted for each condition. 60 contacts between NK cells and H1N1-infected monocytes were observed and LFA-1 accumulation was used to identify immune synapse formation in a blinded fashion **(H)**. The percentage of immune synapse for each condition is represented. **P<0.01 and ***P<0.001 (Wilcoxon matched-paired test to compare each condition).

Figure 6. CD38 contributes to immune synapse formation between NK cells and cancer cells.

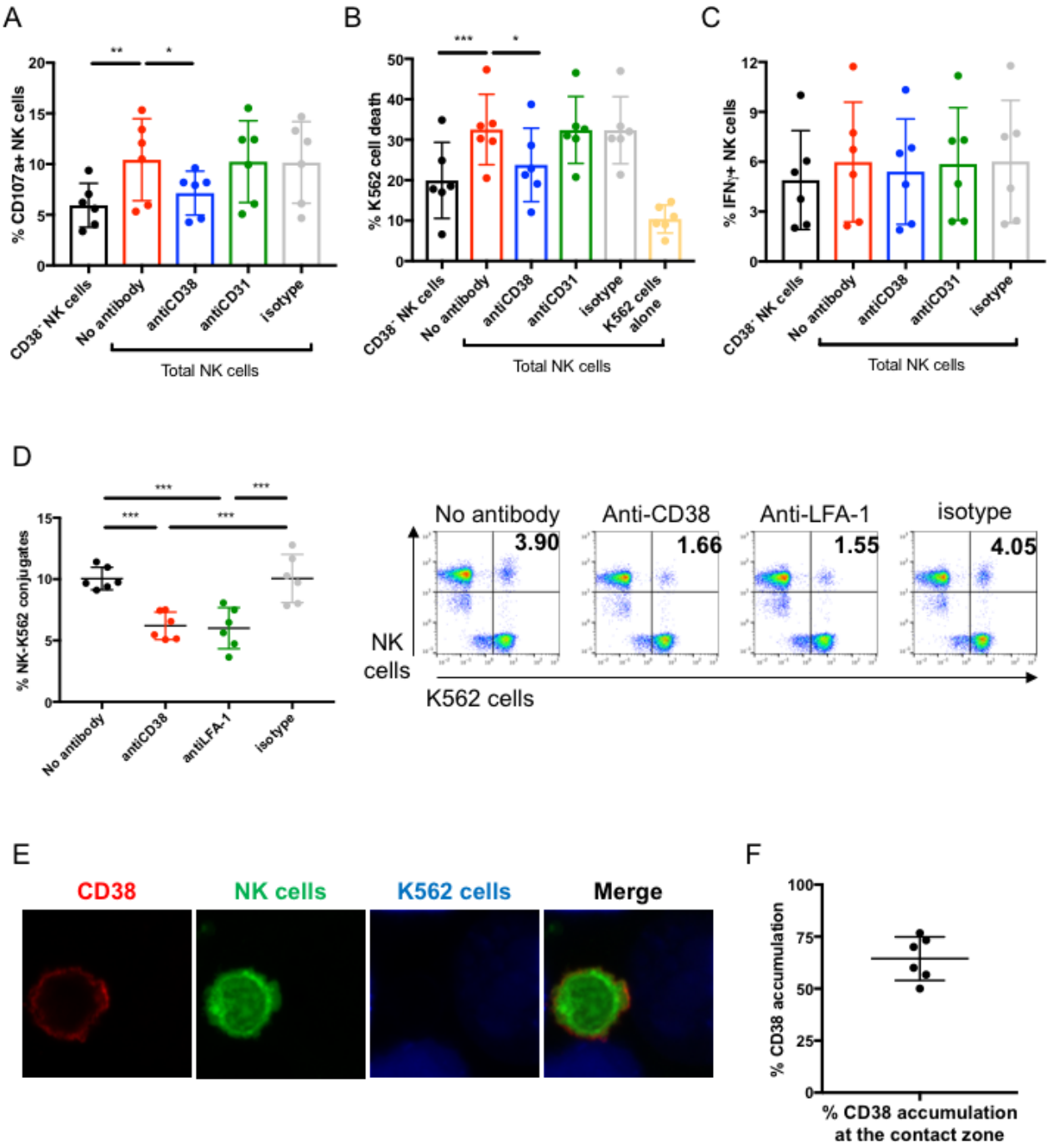

(A to C) from PBMCs from healthy blood donors (N=6) were collected, CD38$^-$ or total NK cells were sorted, incubated with an isotype control (grey dots), CD38 (blue dots) or CD31 (green dots) blocking antibody or without antibody (red dots), and exposed to K562 tumor cells for 4h. CD107a expression **(A)**, K562 cell killing **(B)** and IFN-γ production **(C)** by NK cells was measured by flow cytometry. *P<0.05, **P<0.01, ***P<0.001 (Wilcoxon matched-paired test). **(D)** NK cells from 6 healthy donors were isolated

and stained with CFSE. In parallel, K562 cells were stained with Cell Trace Violet. NK cells were then exposed to K562 cells for 0 or 40 min in presence or absence of a CD38 or LFA-1 blocking antibody or an isotype control antibody. NK cell-K562 cell conjugation was determined by the accumulation of the double positive $CFSE^{+}$Cell Trace $Violet^{+}$ population by flow cytometry. Left graph represents a summary of the experiment and the right panel shows representative plots from one individual. ***P<0.001 (Wilcoxon matched-paired test). **(E and F)** Total NK cells from healthy blood donors (N=6) were isolated and exposed to K562 tumor cells for 1h. **(E)** CD38 (in red) and LFA-1 (in green) localization was determined by confocal microscopy. A representative image is depicted for each condition. **(F)** Accumulation of CD38 in 30 contact zones between NK and K562 cells was determined. The percentage of CD38 accumulation at the contact zone was determined.

769 **Supplemental Materials.**

770 **Figure S1. NK cell gating strategy.**

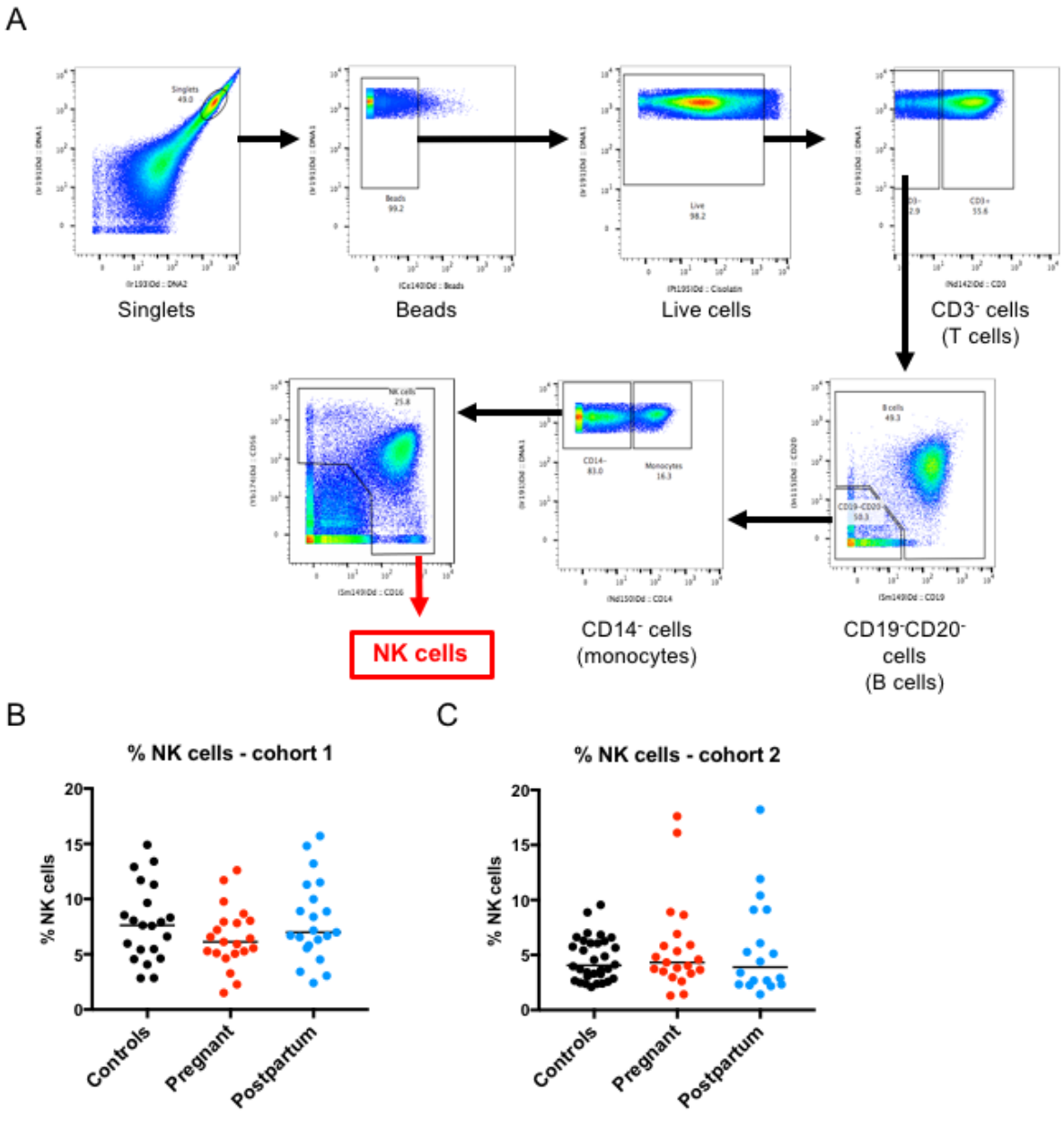

771

772 **(A)** Two-dimensional mass cytometry plots are shown for a representative patient sample. Gating was
773 performed using FlowJo software (FlowJo, LLC). Negative lineage gating was performed to exclude CD3+
774 T cells, CD19+CD20+ B cells and CD14+ monocytes, followed by a positive gating on $CD56^{+/-}CD16^{+/-}$ NK
775 cells. **(B and C)** Percentage of NK cells within PBMCs of controls, pregnant women and postpartum in
776 cohort 1 **(B)** and cohort 2 **(C)**.

777

778 **Figure S2. CD38 expression in control, pregnant and postpartum women from cohort 1 and 2.**

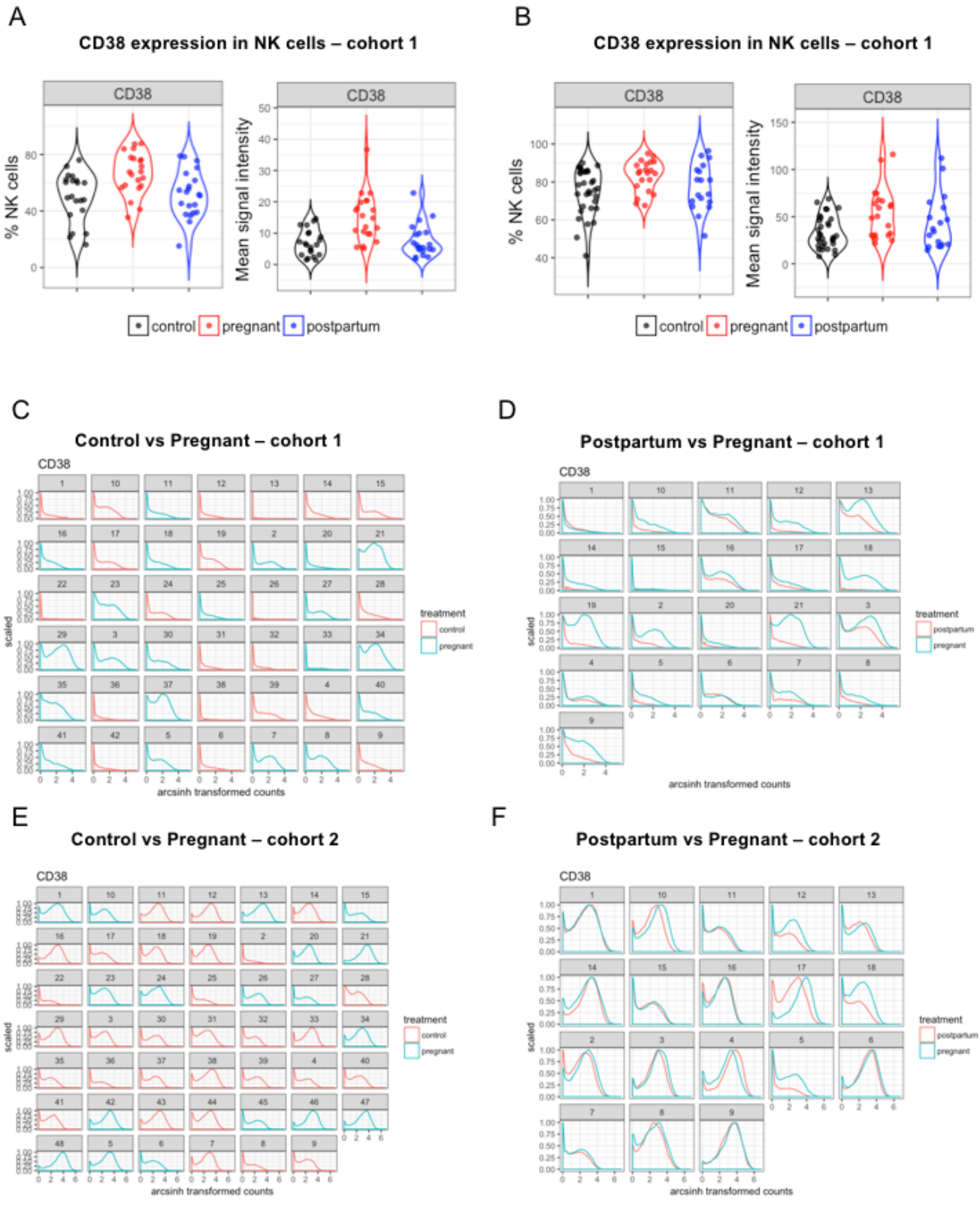

779

780 **(A and B)** Manual gating for CD38 expression on NK cells in control, pregnant and postpartum women in

781 cohort 1 **(A)** and 2 **(B)**. The left panel represents the percent of $CD38^{+}$ NK cells and the right panel represents

782 CD38 mean signal intensity. **(C to F)** NK cells from control and pregnant women (**C**, for cohort 1 and **E**,
783 for cohort 2), pregnant women and postpartum (**D**, for cohort 1 and **F**, for cohort 2) were analyzed and
784 expression of CD38 was measured and shown as density plots.
785

Figure S3. Gating strategy for each marker on NK cells from cohort 1.

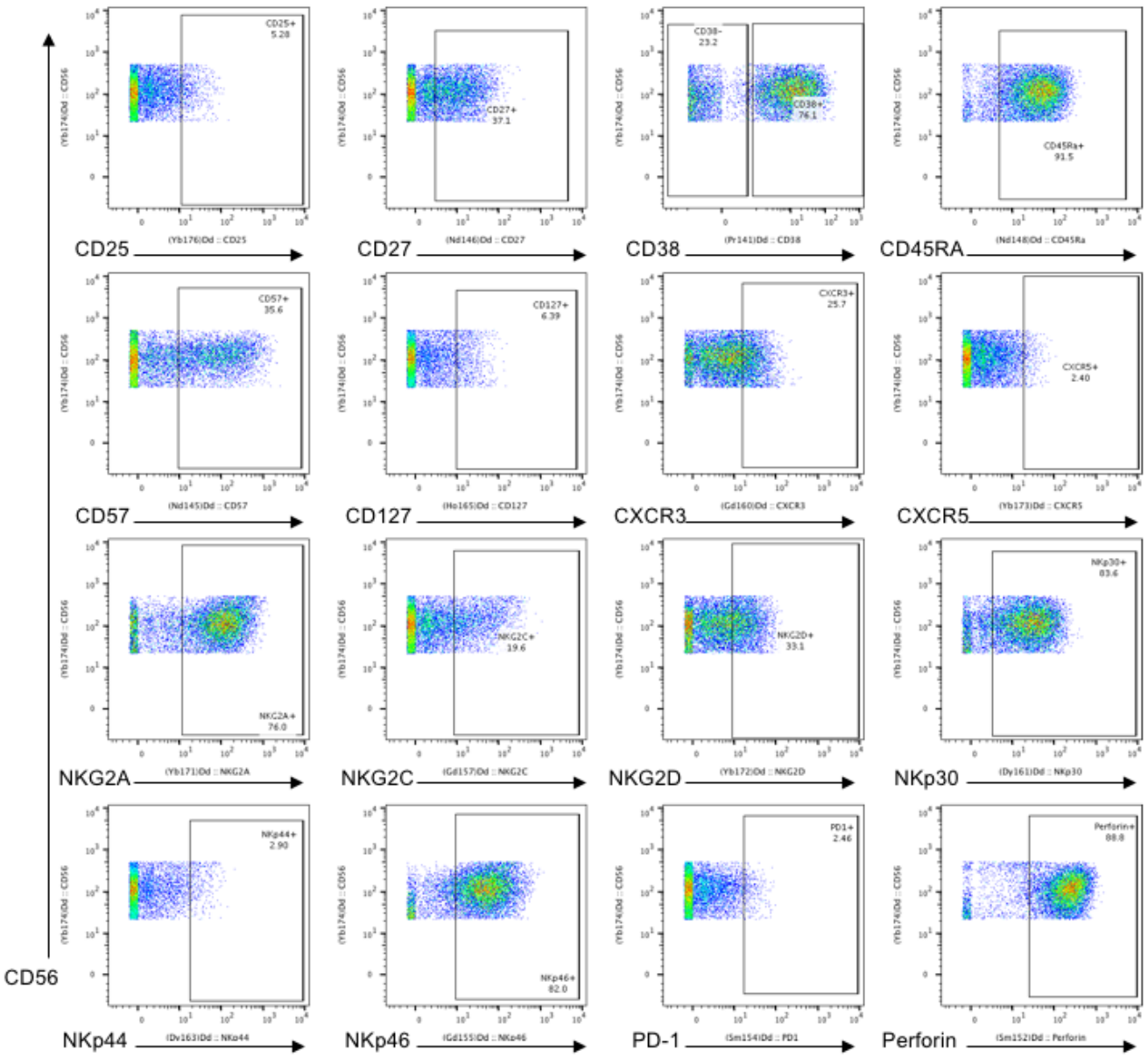

Representative plots for each marker are shown.

790 **Figure S4. Gating strategy for each marker on NK cells from cohort 2.**

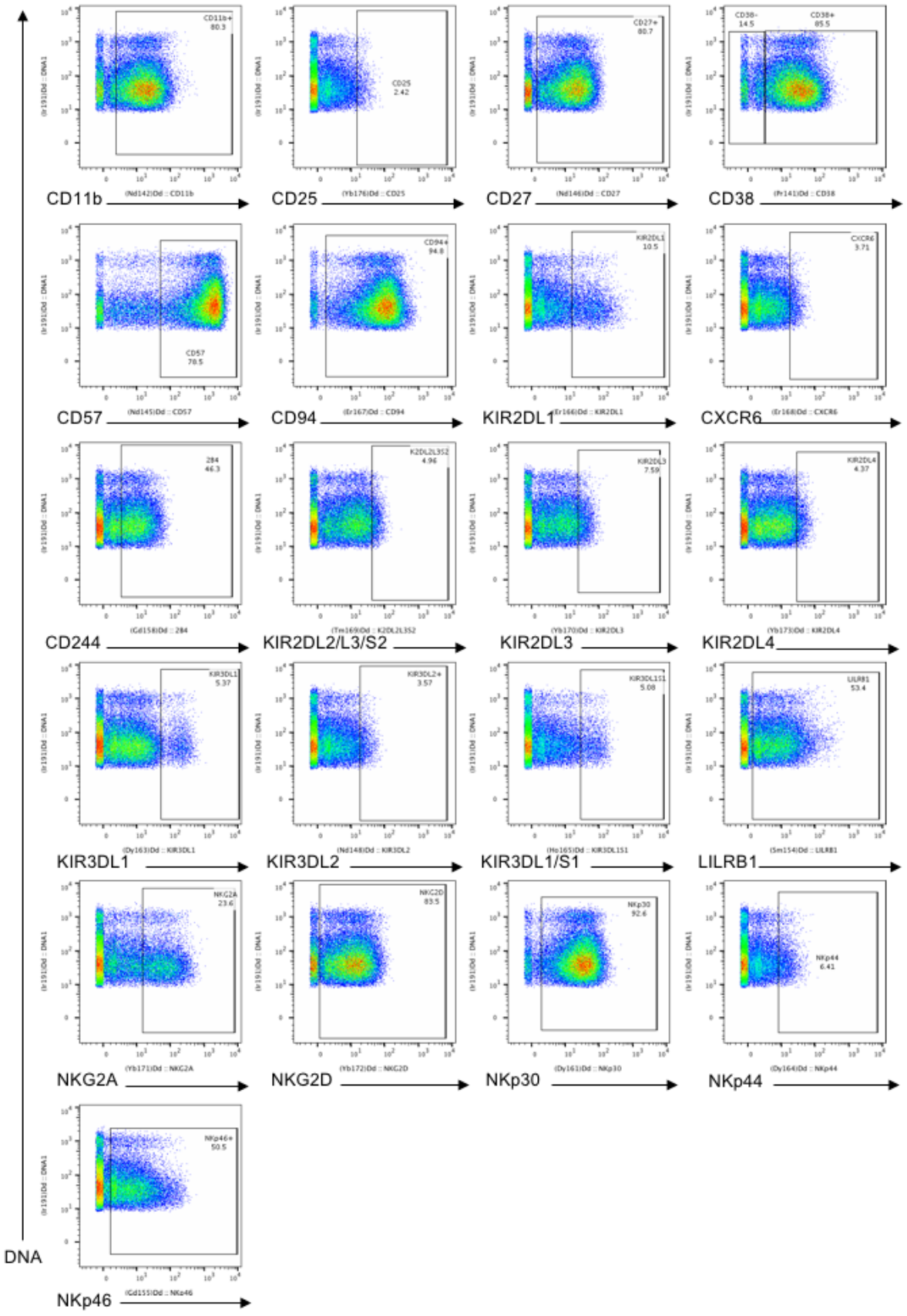

791

792 Representative plots for each marker are shown.

Figure S5. Percentage of expression for each marker on NK cells from cohort 1 and 2 using conventional gating.

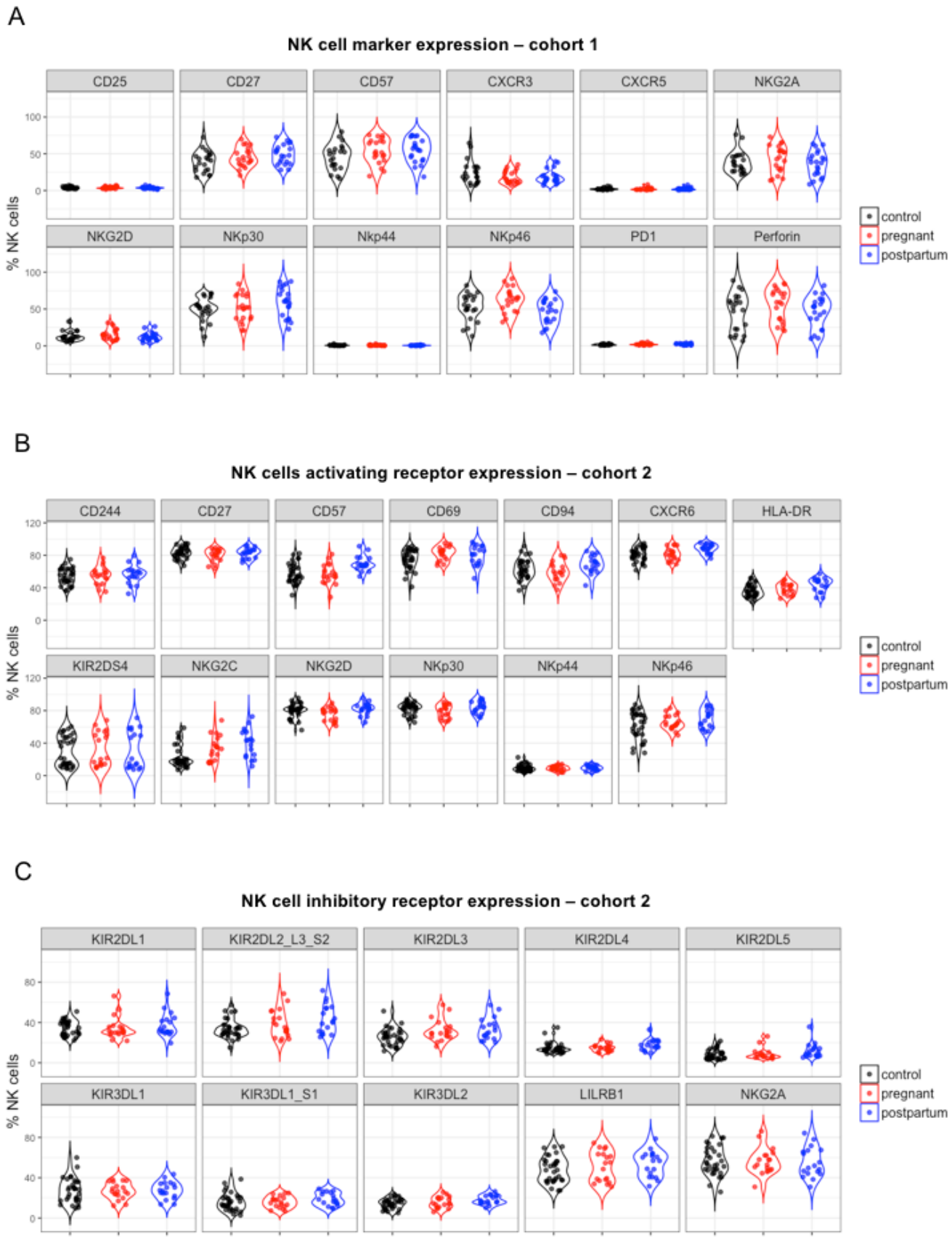

796 **(A to C)** NK cells from controls and pregnant women, as well as postpartum on cohort 1 and 2 were isolated
797 and stained using a 22- or 31 parameter antibody panel, respectively. Percentage of each marker on NK
798 cells was determined by conventional gating for cohort 1 **(A)** and 2 **(B and C)**.
799

Figure S6. Mean Signal intensity of NK cell markers in control, pregnant and postpartum from cohort 1 using conventional gating.

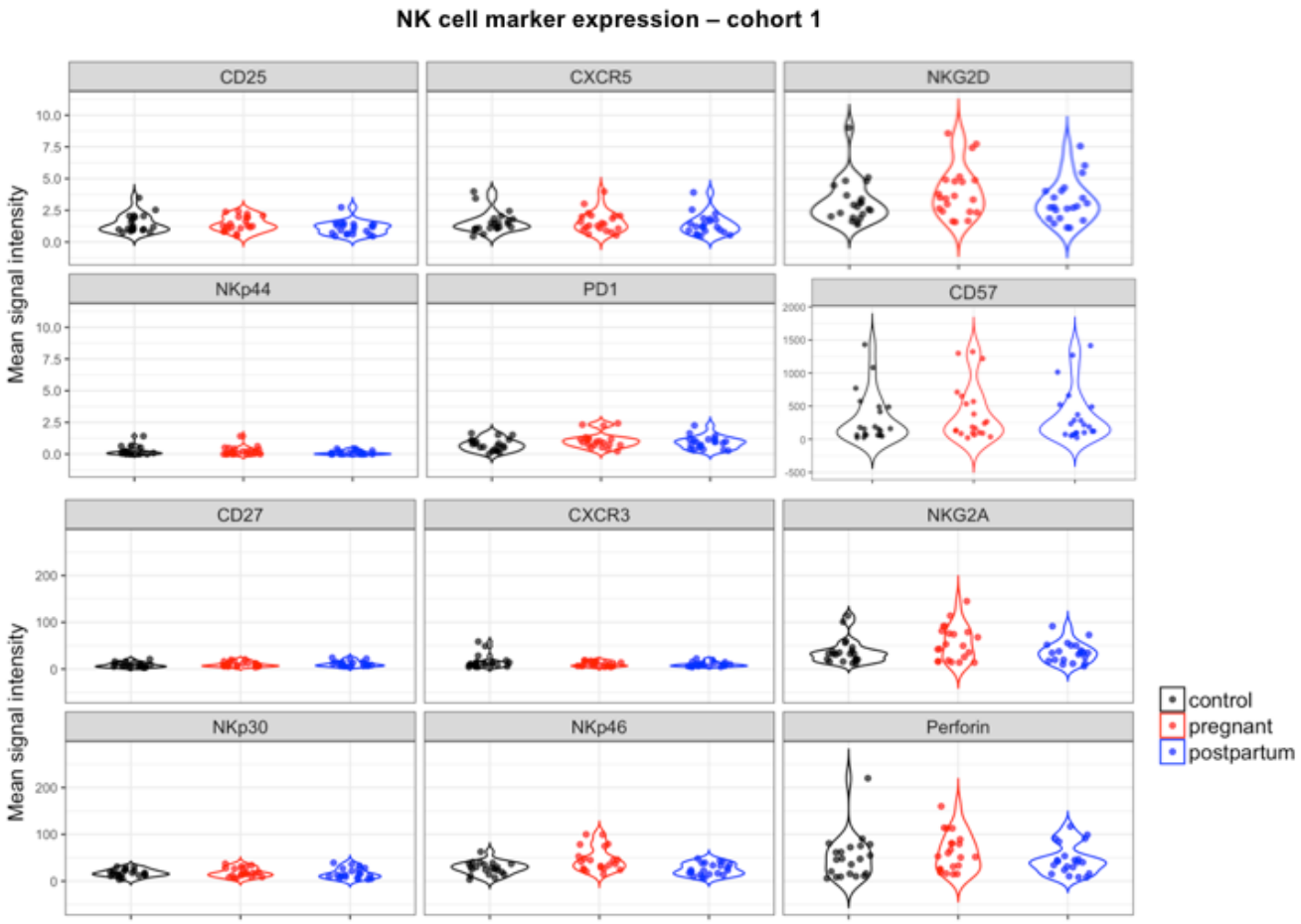

NK cells from controls, pregnant, and postpartum women from cohort 1 were isolated and stained using a 22-parameter antibody panel. Mean Signal Intensity for each marker was determined by conventional gating.

Figure S7. Mean Signal intensity of NK cell markers in control, pregnant and postpartum from cohort 2 using conventional gating.

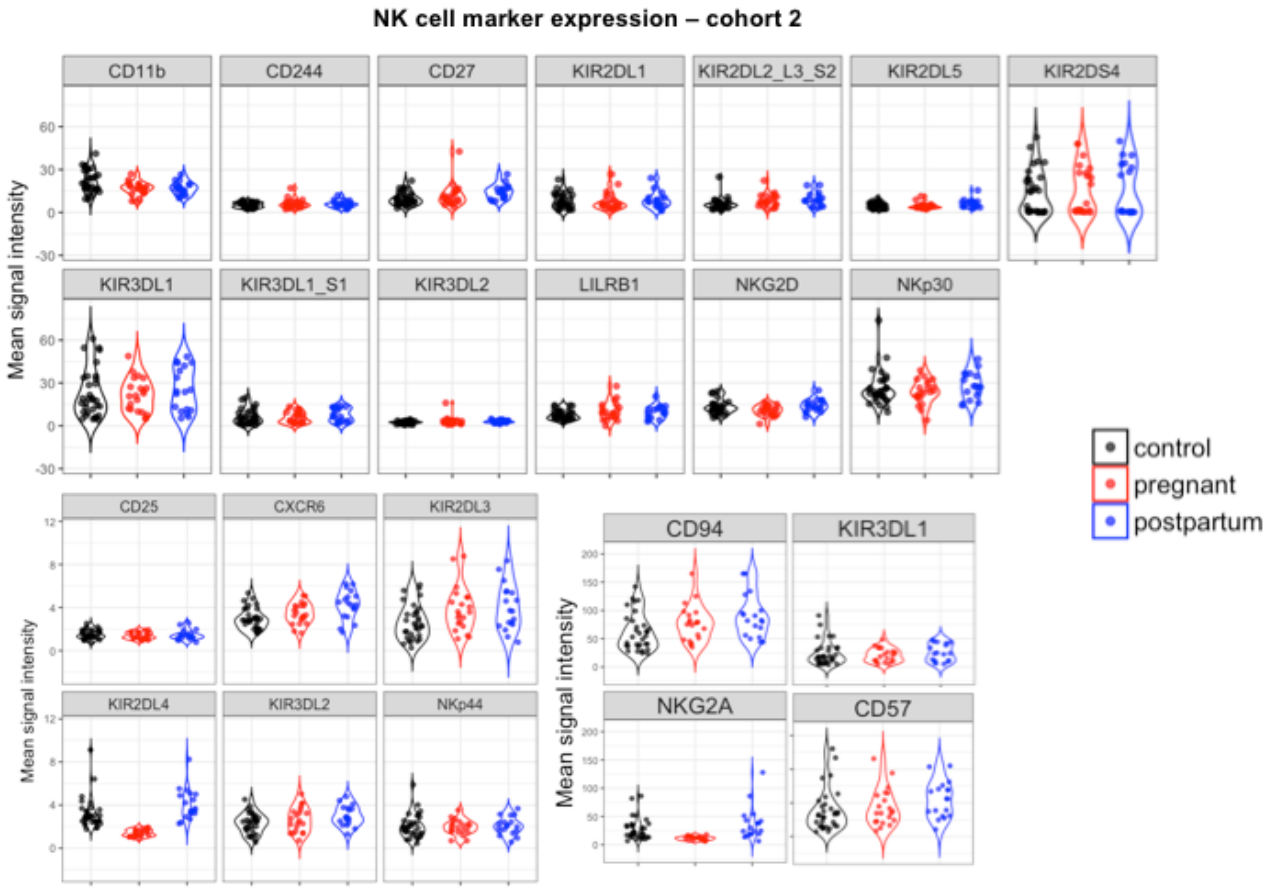

NK cells from controls, pregnant, and postparum women in cohort 2 were isolated and stained using a 31-parameter antibody panel. Mean Signal Intensity for each marker was determined by conventional gating.

Figure S8. Comparison of CD38⁻ and CD38⁺ NK cell expression of each marker in control and pregnant women from cohort 1 using logistic regression model and conventional gating.

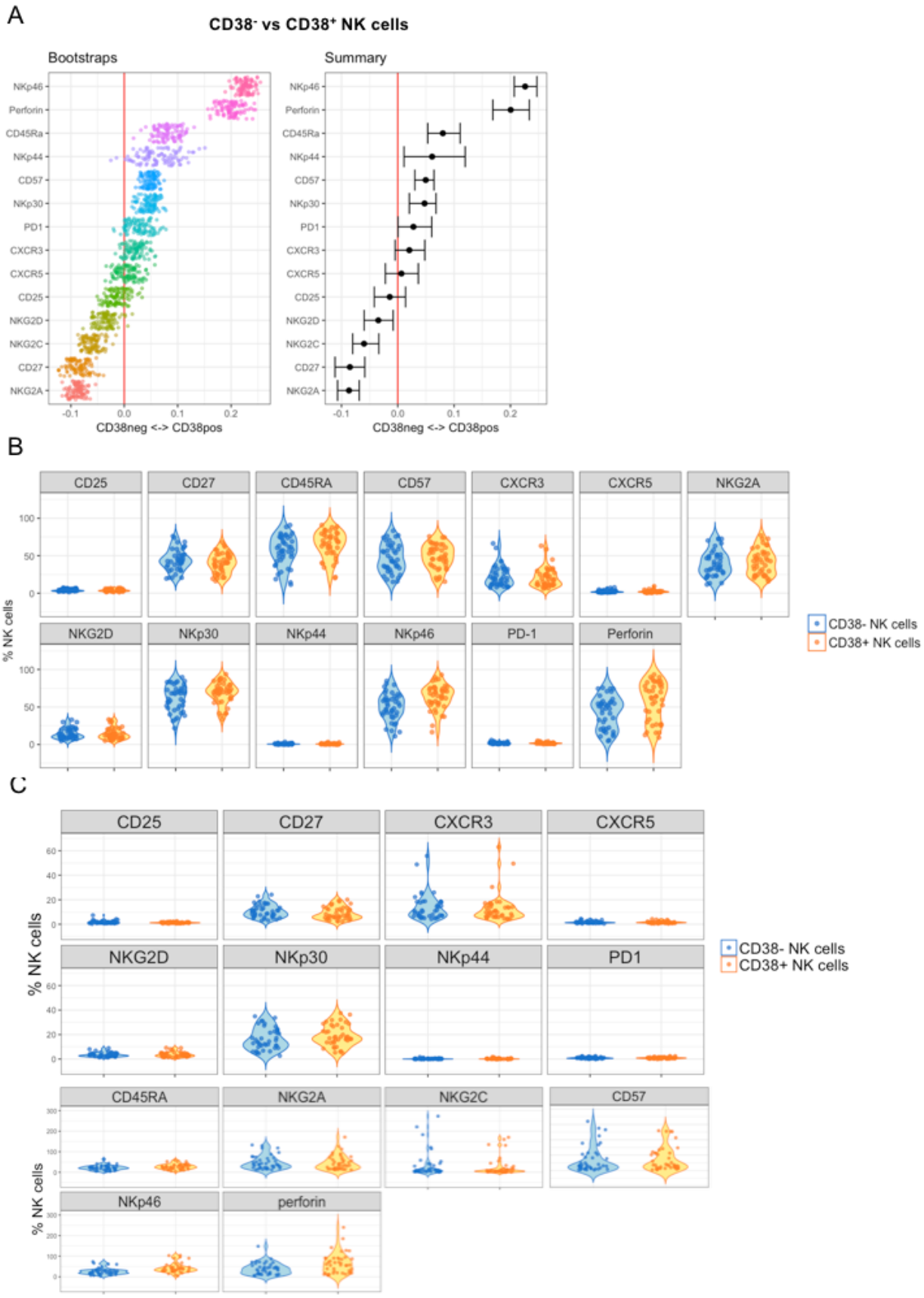

816 **(A to C)** PBMCs from control and pregnant women in cohort 1 were stained using specific NK cell
817 antibodies without stimulation and acquired through a mass cytometer. Data from control and pregnant
818 women were pooled and analyzed using a logistic regression model **(A)** showing whether each NK cell
819 marker is predictive of $CD38^-$ or $CD38^+$ NK cells. Pooled data were also analyzed by conventional gating
820 to determine the percentage of **(B)** and mean signal expression **(C)** for each marker on $CD38^-$ or $CD38^+$ NK
821 cells.
822

Figure S9. Comparison of activating and inhibitory receptor expression on CD38$^-$ and CD38$^+$ NK cells from cohort 2 in control or pregnant women by conventional gating.

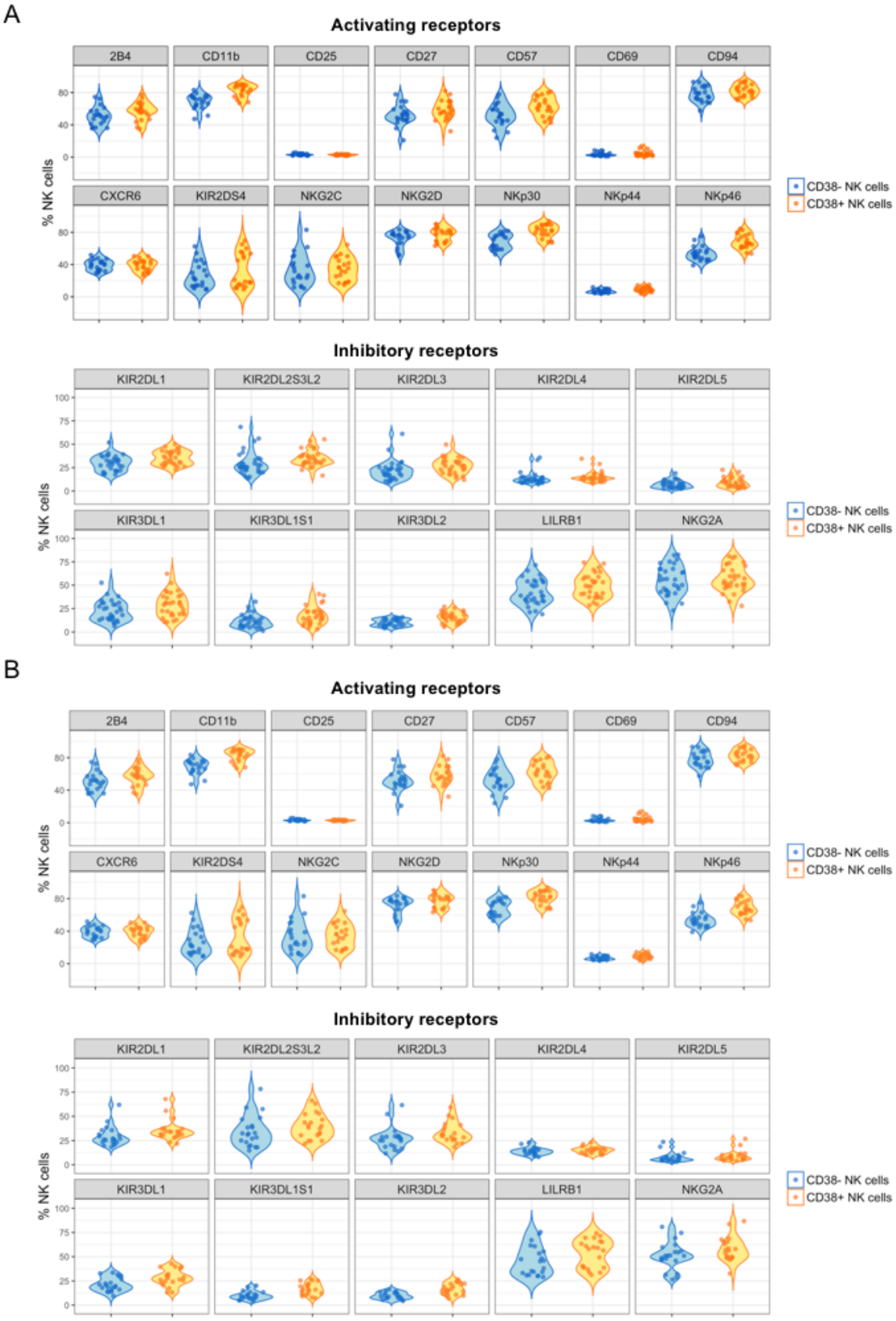

826 **(A and B)** PBMCs from control and pregnant women were stained using specific NK cell antibodies
827 without stimulation and acquired through a mass cytometer. **(A)** Percentage of expression of activating and
828 inhibitory receptors on $CD38^-$ and $CD38^+$ NK cells from control. **(B)** Percentage of expression of activating
829 and inhibitory receptors on $CD38^-$ and $CD38^+$ NK cells from pregnant women.
830

Figure S10. Effect of the CD38 enzyme inhibitor, kuromanin, on the NK cell response to H1N1-infected monocytes.

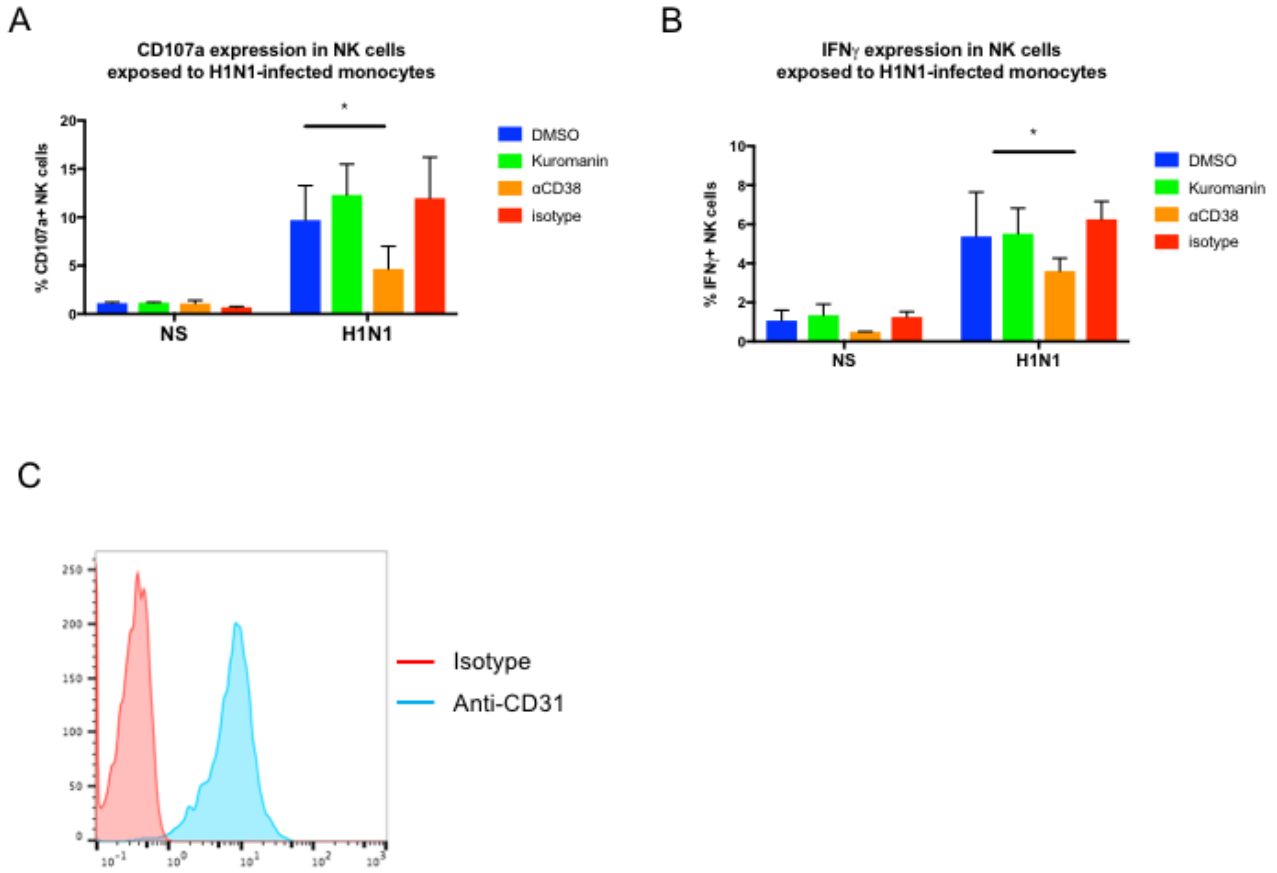

NK cells and monocytes from healthy blood donors (N=6) were isolated and monocytes were infected by H1N1 virus. Autologous NK cells were exposed to infected monocytes in presence of isotype or CD38 blocking antibody, or kuromanin. CD107a **(A)** and IFN-γ **(B)** expression was then measured by flow cytometry. **(C)** CD31 measured expression by flow cytometry in non-infected monocytes. *P<0.05 (Wilcoxon matched-paired test to compare $CD38^-$ and $CD38^+$ NK cells).

Figure S11. CD38 contributes to NK cell-influenza-infected monocytes conjugation.

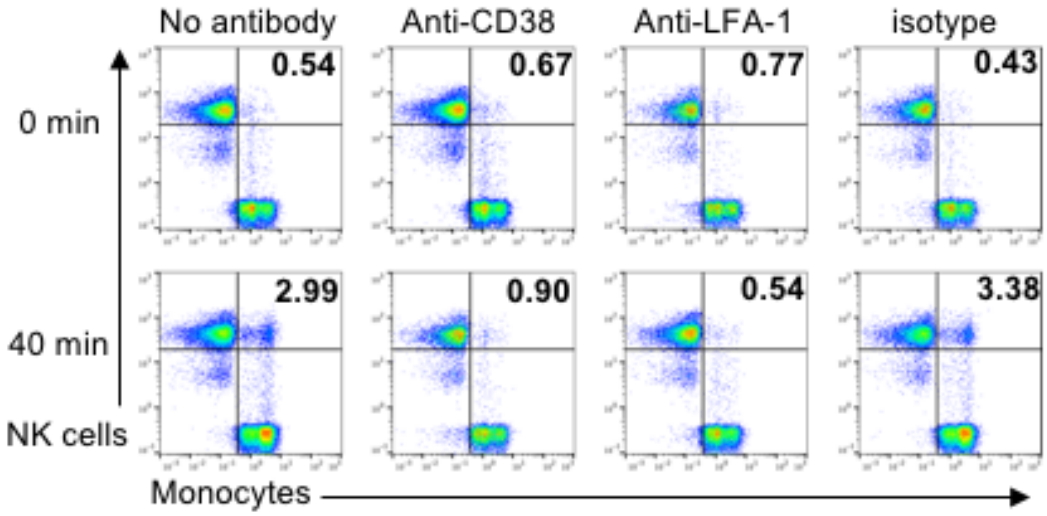

NK cells and monocytes were isolated from healthy donors (N=6). NK cells and monocytes were stained with CFSE and Cell Trace Violet, respectively. Monocytes were infected by H1N1 virus. NK cells were incubated with a CD38 or LFA-1 blocking antibody, an isotype control antibody or no antibody. NK cells were then exposed to H1N1-infected monocytes for 0 or 40 min. NK cell-monocyte conjugation was determined by the accumulation of the double positive $CFSE^{+}CellTrace\ Violet^{+}$ population by flow cytometry. Representative plots from an individual are depicted.

Table S1. Demographics for cohort 1.

Characteristic	Pregnant, n = 21	Control, n=21
Age, years (median)	*30.0 (21 to 42)*	*27.2 (19 to 43)*
White, n (%)	*4 (19)*	11 (52)
Asian, n (%)	*4 (19)*	*5 (24)*
Hispanic, n (%)	*9 (43)*	*3 (14)*
Race, other, n (%)	*4 (19)*	*1 (5)*
Trimester 2, n (%)	*10 (48)*	
Trimester 3, n (%)	*11 (52)*	

Table S2 Demographics for Cohort 2

Characteristic	Pregnant, n = 21	Control, n=32
Age, years (median)	*29.2 (19 to 40)*	*36.8 (19 to 44)*
White, n (%)	*4 (19)*	20 (62)
Asian, n (%)	*4 (19)*	*6 (18)*
Hispanic, n (%)	*9 (43)*	*5 (15)*
Race, other, n (%)	*4 (19)*	*1(3)*
Trimester 2, n (%)	*10 (48)*	
Trimester 3, n (%)	*11 (52)*	

858 **Table S3.** Antibody panel for mass cytometry in cohort 1.
859

Isotope	Antigen	Clone
115In	CD20	2H7
141Pr	CD38	HIT2
142Nd	CD3	UCHT1
145Nd	CD57	HCD57
146Nd	CD27	O323
148Nd	CD45Ra	HI100
149Sm	CD19	HIB19
150Nd	CD14	M5E2
152Sm	Perforin	B-D48
154Sm	PD1	EH12.2H7
155Gd	NKp46	9E2/NKp46
157Gd	NKG2C	134591
159Tb	CD16	3G8
160Gd	CXCR3	G025H7
161Dy	NKp30	P30-15
163Dy	NKp44	P44-8
165Ho	CD127	A019D5
171Yb	NKG2A	Z199
172Yb	NKG2D	1D11
173Yb	CXCR5	51505
174Yb	CD56	NCAM16.2
176Yb	CD25	M-A251
191Ir	DNA1	
193Ir	DNA2	
195Pt	Cisplatin	

860

861

862 **Table S4.** Antibody panel for mass cytometry in cohort 2.
863

Isotope	Antigen	Clone
115Ln	CD20	2H7
141Pr	CD38	HIT2
142Nd	CD11b	ICRF44
145Nd	CD57	HCD57
146Nd	CD27	O323
147Sm	CD127	A019D5
149Sm	CD16	3G8
150Nd	CD14	M5E2
151Eu	CD19	HIB19
152Sm	CD15	W6D3
153Eu	KIR2DS4	179315
154Gd	LILRB1	GHI/75
155Gd	NKp46	9E2/NKp46
156Gd	CD3	UCHT1
157Gd	NKG2C	134591
158Gd	CD244	2-69
159Tb	CD33	WM53
161Dy	NKp30	P30-15
163Dy	KIR3DL1	DX9
164Dy	NKp44	P44-8
165Ho	KIR3DL1_S1	REA168
166Er	KIR2DL1	143211
167Er	CD94	DX22
168Er	CXCR6	56811
169Tm	KIR2DL2_L3_S2	DX27
170Yb	KIR2DL3	180701
171Yb	NKG2A	Z199
172Yb	NKG2D	1D11
173Yb	KIR2DL4	mAB 33
174Yb	CD56	NCAM16.2
176Yb	CD25	M-A251
191Ir	DNA1	
193Ir	DNA2	
195Pt	Cisplatin	

864